

# The Cell Motility Modulator Slit2 Is a Potent Inhibitor of Platelet Function

Sajedabanu Patel, MSc; Yi-Wei Huang, PhD; Adili Reheman, MD; Fred G. Pluthero, PhD;  
Swasti Chaturvedi, MSc, MBBS; Ilya M. Mukovozov, MSc; Soumitra Tole, MSc;  
Guang-Ying Liu, MD; Ling Li, MSc; Yves Durocher, PhD; Heyu Ni, MD, PhD;  
Walter H.A. Kahr, MD, PhD; Lisa A. Robinson, MD

**Background**—Vascular injury and atherothrombosis involve vessel infiltration by inflammatory leukocytes, migration of medial vascular smooth muscle cells to the intimal layer, and ultimately acute thrombosis. A strategy to simultaneously target these pathological processes has yet to be identified. The secreted protein, Slit2, and its transmembrane receptor, Robo-1, repel neuronal migration in the developing central nervous system. More recently, it has been appreciated that Slit2 impairs chemotaxis of leukocytes and vascular smooth muscle cells toward diverse inflammatory attractants. The effects of Slit2 on platelet function and thrombus formation have never been explored.

**Methods and Results**—We detected Robo-1 expression in human and murine platelets and megakaryocytes and confirmed its presence via immunofluorescence microscopy and flow cytometry. In both static and shear microfluidic assays, Slit2 impaired platelet adhesion and spreading on diverse extracellular matrix substrates by suppressing activation of Akt. Slit2 also prevented platelet activation on exposure to ADP. In in vivo studies, Slit2 prolonged bleeding times in murine tail bleeding assays. Using intravital microscopy, we found that after mesenteric arteriolar and carotid artery injury, Slit2 delayed vessel occlusion time and prevented the stable formation of occlusive arteriolar thrombi.

**Conclusions**—These data demonstrate that Slit2 is a powerful negative regulator of platelet function and thrombus formation. The ability to simultaneously block multiple events in vascular injury may allow Slit2 to effectively prevent and treat thrombotic disorders such as myocardial infarction and stroke. (*Circulation*. 2012;126:1385-1395.)

**Key Words:** blood cells ■ blood platelets ■ thrombosis

Cardiovascular disease leading to heart attack and stroke remains the leading cause of mortality and morbidity in the Western world.<sup>1,2</sup> Atherosclerosis is a progressive disease characterized by accumulation of inflammatory cells and vascular smooth muscle cells (VSMCs) within the intima of injured blood vessels. The atherosclerotic plaque is made up of immune cells, including monocytes, macrophages, neutrophils, T lymphocytes, and VSMCs, that migrate from the media to the intima where they proliferate and secrete extracellular matrix proteins. Platelets have also been implicated in the initiation of atherosclerotic lesion formation.<sup>3,4</sup> These events result in progressive narrowing of the vessel, allowing platelet aggregation and activation to ultimately

form vascular occlusive thrombi, precipitating acute coronary syndromes and ischemic stroke.<sup>5</sup>

## Clinical Perspective on p 1395

Strategies that block recruitment to the intima of immune cells and VSMCs are partially protective against vascular injury in both animal models and human patients. Inhibiting monocyte and VSMC recruitment to selected chemoattractants partially prevents atherosclerosis and its clinical manifestations, and simultaneous blockade of 2 chemotactic pathways confers additional, but not complete, benefit.<sup>2,6</sup> Medical therapies that inhibit platelet activation and aggregation are a mainstay of treatment for

Received August 25, 2011; accepted July 19, 2012.

From the Program in Cell Biology, The Hospital for Sick Children Research Institute, Toronto, ON, Canada (S.P., Y.-W.H., F.G.P., S.C., I.M.M., S.T., G.-Y.L., L.L., W.H.A.K., L.A.R.); Institute of Medical Science, University of Toronto, Toronto, ON, Canada (S.P., S.C., I.M.M., W.H.A.K., L.A.R.); Department of Laboratory Medicine, Keenan Research Center, Li Ka Shing Knowledge Institute, St. Michael's Hospital, and Toronto Platelet Immunobiology Group, Toronto, ON, Canada (A.R., H.N.); Biotechnology Research Institute, National Research Council Canada, Montreal, QC, Canada (Y.D.); Canadian Blood Services, Toronto, ON, Canada (H.N.); and Department of Paediatrics, Division of Haematology/Oncology (W.H.A.K.), and Department of Paediatrics, Division of Nephrology (L.A.R.), The Hospital for Sick Children, University of Toronto, Toronto, ON, Canada.

The online-only Data Supplement is available with this article at <http://circ.ahajournals.org/lookup/suppl/doi:10.1161/CIRCULATIONAHA.112.105452/-/DC1>.

Correspondence to Lisa A. Robinson, MD, The Hospital for Sick Children, 555 University Ave, Room 5265, Toronto, ON, Canada M5G 1X8. E-mail [lisa.robinson@sickkids.ca](mailto:lisa.robinson@sickkids.ca)

© 2012 American Heart Association, Inc.

*Circulation* is available at <http://circ.ahajournals.org>

DOI: 10.1161/CIRCULATIONAHA.112.105452

patients at risk for cardiovascular events, making antiplatelet agents the most widely prescribed drugs worldwide.<sup>1</sup> However, these agents also provide only partial protection against cardiovascular events.

Given the variety of infiltrating cell types and molecular migration cues involved in atherogenesis, it is unlikely that targeting a single chemoattractant pathway will achieve widespread clinical success. Rather, generalized blockade of harmful cell migration cues, combined with platelet inhibition within the vasculature, would be more beneficial.

The Slit family of secreted proteins, together with their transmembrane receptor, Roundabout (Robo), act as repellents for migrating neurons and axons during the development of the central nervous system.<sup>7–9</sup> It has recently been appreciated that Slit and Robo are also expressed in mature organisms, and an isoform of Robo, Robo-1, has been detected on the surface of several cell types involved in vascular injury and atherogenesis, including VSMCs, neutrophils, and mononuclear leukocytes.<sup>10–14</sup> Work from our group and others has shown that Slit2 interacts with Robo-1 to prevent directional migration of these cells in response to diverse inflammatory chemoattractant cues both in vitro and in vivo.<sup>10–15</sup> The possible role of Slit2 in modulating platelet recruitment and activation has heretofore not been explored. We report here that Robo-1 is expressed in megakaryocytes and platelets and is present on the platelet cell surface in humans and mice. We further demonstrate that Slit2 is a potent inhibitor of platelet adhesion, spreading, and activation in response to diverse stimuli in vitro and impairs platelet function and thrombus stability in vivo. These results suggest that Slit2, a naturally occurring protein, has the potential to serve as a therapeutic agent for simultaneously inhibiting the development of atherosclerotic vascular lesions and the acute platelet thrombus that collectively contribute to heart attack and stroke.

## Methods

Detailed methods are available in the online-only Data Supplement.

### Isolation of Human and Murine Platelets

Human washed platelets were isolated from whole blood collected from healthy volunteers into acid citrate dextrose (1 vol). Murine platelets were isolated from blood collected by cardiac puncture in hirudin.

### Statistical Analysis

ANOVA was performed to compare group means in multiple comparisons. In other cases, the Student 2-tailed *t* test was used for comparison of means, or the Fisher exact test was used for comparison of proportions. Values of  $P < 0.05$  were considered significant.

## Results

### Platelets Express Robo-1 on Their Surface

Immunoblot analysis of cell lysates detected expression of the Slit2 receptor, Robo-1, in human platelets and their precursor megakaryocytes (Figure 1A). Laser immunofluorescence confocal microscopy showed that in human and murine platelets, Robo-1 receptors localized to the cell surface (Figure 1B and 1C). Using flow cytometry, we observed that 96% of human platelets expressed Robo-1 (Figure 1D and 1E).

Because the repulsive effects of Slit2 are thought to be mediated by the leucine-rich regions present at the N-terminus, we next examined the binding of a truncated N-terminal preparation of Slit2 (Slit2-N) comprising these leucine-rich regions to the platelet surface.<sup>10,16</sup> Using flow cytometry, we directly demonstrated binding of Slit2-N to Robo-1 on the surface of platelets (Figure 1A, 1B, and 1H in the online-only Data Supplement). To verify that the observed binding of Slit2 was specific, we generated a soluble N-terminal fragment of Robo-1 (RoboN) that binds Slit2, competitively preventing binding of Slit2 to Robo-1 on the cell surface, thereby preventing initiation of downstream signaling events.<sup>17</sup> Using flow cytometry, we demonstrated that RoboN inhibited binding of Slit2-N to the surface of platelets in a dose-dependent manner (Figure 1B–1F and 1H in the online-only Data Supplement). To further verify that the observed effects of Slit2 were not due to nonspecific protein binding, we generated mutant Slit2 protein that lacks the second leucine-rich region that is necessary for binding to Robo-1 (Slit $\Delta$ D2).<sup>16,18</sup> Flow cytometry analysis demonstrated that this mutant Slit2 protein, Slit $\Delta$ D2, did not significantly bind to the surface of platelets (Figure 1G and 1H in the online-only Data Supplement). Furthermore, activation of platelets with the agonist ADP did not significantly alter the binding of Slit2 to the surface of platelets (Figure 1I and 1J in the online-only Data Supplement). Together, these data demonstrate that human and mouse platelets express Robo-1 and that Slit2 directly binds Robo-1 receptors on the platelet surface.

### Slit2 Inhibits Spreading of Human Platelets

The potential effects of Slit2/Robo-1 interactions on platelet function were first examined by assessing the effects of Slit2 on adhesion and spreading of human platelets on a fibrinogen-coated surface. Untreated cells progressively spread on fibrinogen-coated coverslips during a 30-minute observation period (Figure 2A and 2B). In the presence of Slit2, platelet spreading was markedly decreased, with cells exhibiting short, warped filopodia and decreased formation of lamellar sheets (Figure 2A). After 30 minutes, the mean platelet surface area was  $20.9 \pm 2.5 \mu\text{m}^2$  in the presence of Slit2, significantly less than the  $33.4 \pm 0.6 \mu\text{m}^2$  mean surface area observed for untreated cells ( $P < 0.05$ ; Figure 2B). In real-time visualization, when Slit2 was not present, platelets demonstrated smooth, fluid formation of filopodia and lamellipodia (Video I in the online-only Data Supplement). In sharp contrast, Slit2-treated platelets exhibited rounding of the cell body and development of dynamic and motile filopodial structures but limited formation of lamellar sheets between the filopodia (Video II in the online-only Data Supplement).

To determine whether Slit2 selectively inhibits fibrinogen-induced platelet spreading, the effects of Slit2 on platelet spreading on fibronectin and collagen were examined as described above. After 30 minutes, the mean surface area of platelets on fibronectin-coated coverslips was  $19.3 \pm 2.6 \mu\text{m}^2$  in the presence of Slit2, significantly less than untreated cells ( $31.7 \pm 1.8 \mu\text{m}^2$ ;  $P < 0.05$ ; Figure 2C and 2D). On collagen-coated coverslips, the mean surface area was  $13.5 \pm 0.7 \mu\text{m}^2$

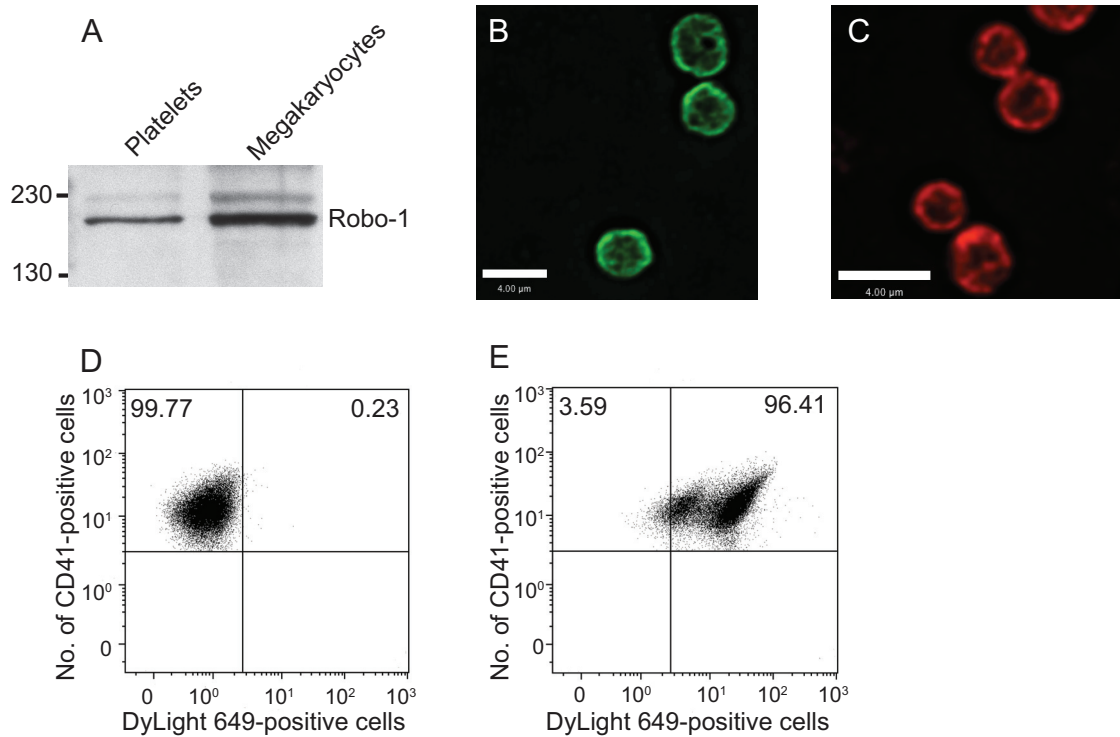


**Figure 1.** Human and murine platelets express Robo-1 on the cell surface. **A**, Cell lysates from normal human platelets and megakaryocytes were subjected to immunoblotting and probed with anti-Robo-1 primary antibody and horseradish peroxidase-conjugated anti-rabbit IgG. **B**, Washed human platelets were fixed, permeabilized, and labeled with anti-Robo-1 antibody followed by Alexa Fluor 488-conjugated anti-rabbit IgG. Image was acquired with a Leica DMIRE2 spinning-disk confocal microscope at  $\times 100$ . Scale bar =  $4 \mu\text{m}$ . **C**, Platelets were isolated from mouse peripheral blood, fixed, permeabilized, and incubated with anti-Robo-1 antibody followed by Alexa Fluor 568-conjugated anti-rabbit IgG. Image was acquired with a Leica DMIRE2 spinning-disk confocal microscope at  $\times 63$ . Scale bar =  $4 \mu\text{m}$ . **D** and **E**, To quantify labeling of Robo-1, human platelets were fixed and labeled with anti-Robo-1 antibody and DyLight 649-conjugated anti-rabbit IgG (**E**) or with secondary antibody alone (**D**). Platelets were concurrently labeled with phycoerythrin-conjugated anti-CD41 antibody. Numbers indicate percentage of cells with positive labeling. Representative images from 1 of 3 similar independent experiments.

in the presence of Slit2, significantly less than that of untreated cells ( $20.8 \pm 1.9 \mu\text{m}^2$ ;  $P < 0.05$ ; Figure 2E and 2F). We next tested whether Slit2-N similarly inhibited platelet spreading.<sup>10,16</sup> After 30 minutes, the mean platelet surface area on fibrinogen-coated surfaces was  $23.3 \pm 0.7 \mu\text{m}^2$  in the presence of Slit2-N, significantly less than the  $36.1 \pm 0.6 \mu\text{m}^2$  mean surface area observed for untreated cells ( $P < 0.01$ ; Figure IIA and IIB in the online-only Data Supplement). To verify that the observed effects of Slit2 were not due to nonspecific protein binding, we also tested platelet spreading with Slit $\Delta$ D2. In the presence of Slit $\Delta$ D2, platelet spreading on fibrinogen was unimpaired (Figure IIA and IIB in the online-only Data Supplement). The mean surface area for platelets treated with Slit $\Delta$ D2 was  $34.9 \pm 0.5 \mu\text{m}^2$ , similar to that of control platelets but significantly higher than that of platelets treated with Slit2-N ( $23.3 \pm 0.7 \mu\text{m}^2$ ;  $P < 0.01$ ; Figure IIA and IIB in the online-only Data Supplement). To further verify that the observed effects of Slit2 on platelet spreading were specific, we used the selective Slit2 antagonist RoboN, a soluble N-terminal fragment of Robo-1. The effects of Slit2 were reversed by RoboN (Figure IIA and IIB in the online-only Data Supplement). The mean surface area for platelets treated with RoboN and Slit2-N was  $34.1 \pm 2.7 \mu\text{m}^2$ , similar to that of control platelets but significantly higher than that of platelets treated with

Slit2-N alone ( $23.3 \pm 0.7 \mu\text{m}^2$ ;  $P < 0.01$ ; Figure IIA and IIB in the online-only Data Supplement). To determine how Slit2 affects the number of platelets adhering to fibrinectin, we performed platelet adhesion assays in 96-well plates. In the presence of Slit2-N, platelet adhesion was reduced by 28% (control,  $7.0 \times 10^4 \pm 0.04 \times 10^4$  cells per well versus Slit2-N,  $5.1 \times 10^4 \pm 0.02 \times 10^4$  cells per well;  $P < 0.01$ ; Figure IIC in the online-only Data Supplement). Collectively, these results demonstrate that Slit2 specifically inhibits platelet adhesion and spreading on diverse substrates.

### Slit2 Inhibits Platelet Adhesion Under Shear Flow Conditions

Collagen is the first potentially activating substrate that platelets typically encounter within an injured blood vessel, and their response is sensitive to shear flow conditions. We used Bioflux microfluidic channels coated with collagen to mimic the hydrodynamic flow conditions that would be encountered by platelets within the arterial circulation.<sup>19</sup> For untreated cells, the average surface area covered by platelets after 4 minutes was  $8.3 \pm 1.3\%$  at a shear flow rate of  $1000 \text{ seconds}^{-1}$  (Figure 3A and 3B). For cells treated with Slit2, this area markedly decreased to  $1.3 \pm 0.5\%$  ( $P < 0.01$ ; Figure 3A and 3B). At a shear flow rate of  $1900 \text{ seconds}^{-1}$ ,

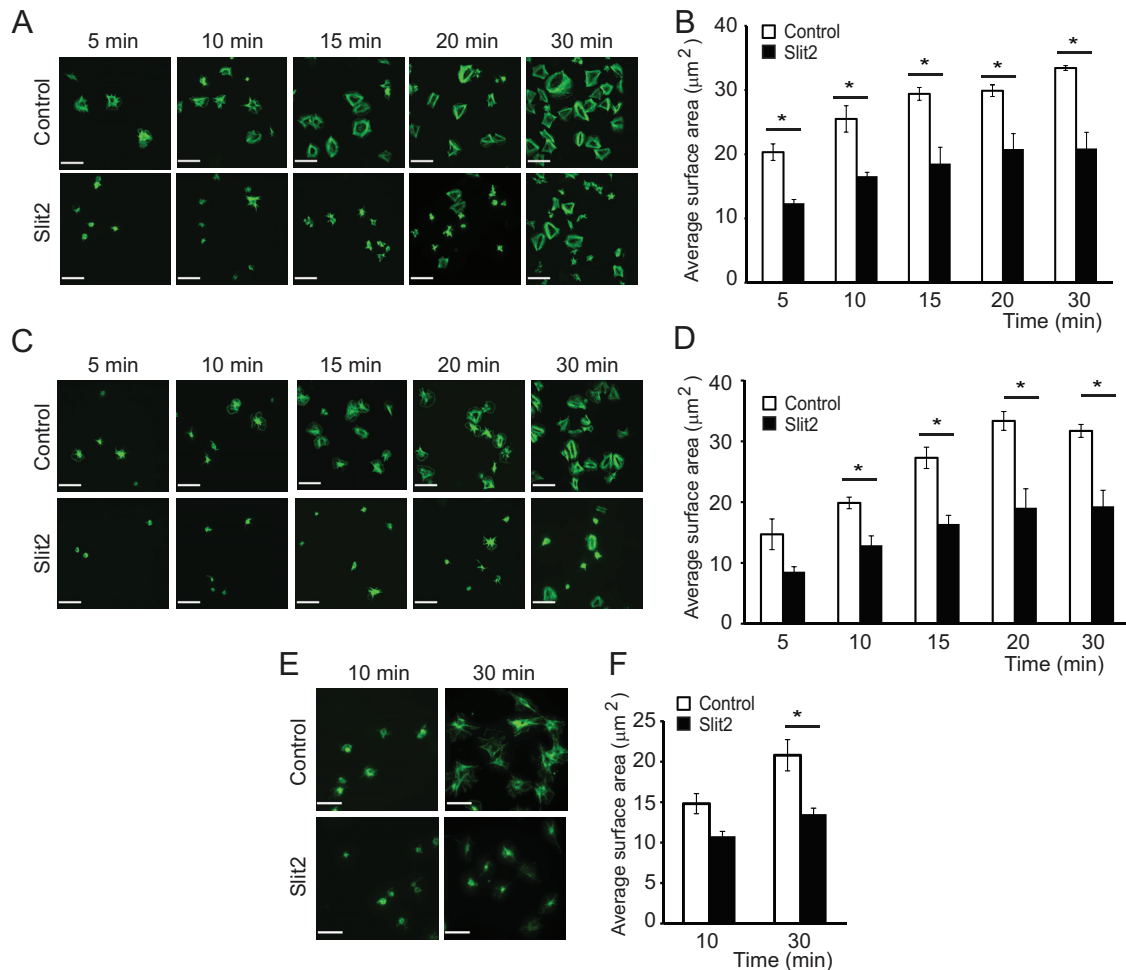


**Figure 2.** Slit2 inhibits human platelet spreading on diverse substrates. Isolated human platelets ( $10^7$  per 1 mL) were preincubated with Slit2 ( $4.5 \mu\text{g/mL}$ ) or an equal volume of PBS (control) for 10 minutes at  $37^\circ\text{C}$  and dispensed onto coverslips precoated with fibrinogen (**A** and **B**), fibronectin (**C** and **D**), or collagen (**E** and **F**) for the indicated times. **A**, Platelets adherent to fibrinogen were fixed, permeabilized, incubated with Alexa Fluor 488–conjugated phalloidin, and visualized with a Leica DMIRE2 spinning-disk confocal microscope. Scale bars= $11 \mu\text{m}$ . **B**, Experiments were performed as in **A**. Images were acquired from 15 random fields, and the surface area of platelets was quantified with Volocity software. Data are expressed as mean $\pm$ SEM from 3 to 5 independent experiments. **C**, Experiments were performed as in **A** using coverslips coated with fibronectin. **D**, Experiments were performed as in **C** and quantification was done as described in **B**. Data are expressed as mean $\pm$ SEM from 3 to 5 independent experiments. **E**, Experiments were performed as in **A** using coverslips coated with collagen. **F**, Experiments were performed as in **E** and quantification was done as described in **B**. Data are expressed as mean $\pm$ SEM from 3 to 5 independent experiments. \* $P<0.05$ .

comparable to hydrodynamic conditions encountered within large arteries, the average platelet surface area coverage decreased 4-fold from  $12.0\pm 2.4\%$  to  $3.1\pm 0.9\%$  on exposure to Slit2 ( $P<0.05$ ; Figure 3A and 3C and Videos III and IV in the online-only Data Supplement). In the presence of Slit2-N, we observed a decrease in platelet adhesion comparable to that seen with full-length Slit2 protein (control,  $8.7\pm 1.4\%$  versus Slit2-N,  $2.5\pm 0.5\%$ ; Figure IIIA and IIIB in the online-only Data Supplement;  $P<0.05$ ). To verify the specificity of Slit2-induced responses, we incubated platelets with Slit $\Delta$ D2, which lacks the Robo-1–binding domain. Platelet adhesion was no different in the presence of Slit $\Delta$ D2 than control platelets but was significantly higher than adhesion of platelets treated with Slit2-N (control,  $8.7\pm 1.4\%$ ; Slit2-N,  $2.5\pm 0.5\%$ ; Slit $\Delta$ D2,  $9.2\pm 1.9\%$ ; Slit $\Delta$ D2 versus Slit2-N,  $P<0.05$ ; Figure IIIA and IIIB in the online-only Data Supplement). Taken together, these data demonstrate that

Slit2 specifically inhibits platelet adhesion under shear flow conditions.

### Slit2 Does Not Affect Rac1 and Cdc42 Activation During Platelet Spreading

Slit2 has been shown to prevent chemotactic migration of various cell types by preventing activation of the Rho-family GTPases, Cdc42, and Rac.<sup>10,12,13,15</sup> To determine whether Slit2 inhibits platelet adhesion and spreading in a similar manner, we used glutathione-S-transferase beads conjugated to the p21-binding domain of PAK1 to detect the activated GTP-bound species of Cdc42 and Rac.<sup>13</sup> Because the predominant isoform of Rac in human platelets is Rac1, we specifically studied the effects of Slit2 on Rac1 activation.<sup>20</sup> Unstimulated platelets exhibited low basal levels of activated Rac1 and Cdc42 (Figure 4A and 4B), and as expected, platelet spreading on fibrinogen increased the levels of

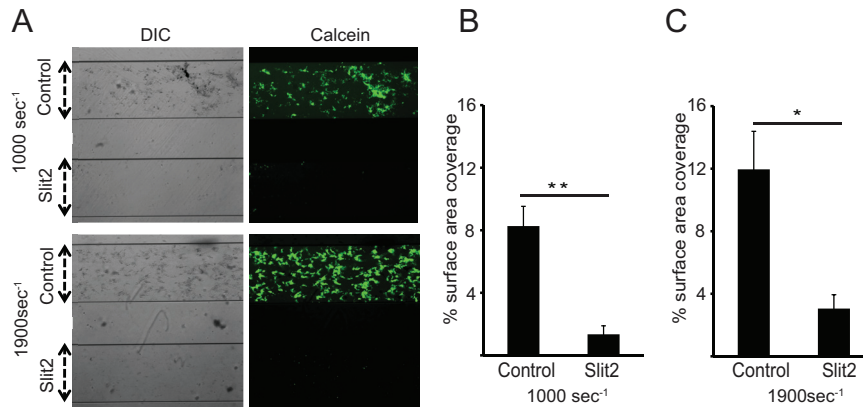


**Figure 3.** Slit2 inhibits platelet adhesion to collagen under shear flow conditions. **A**, Washed human platelets were incubated with calcein-AM for 20 minutes and preincubated with Slit2 (4.5  $\mu\text{g}/\text{mL}$ ) or an equal volume of PBS (control) for 10 minutes at 37°C. Platelets were perfused over collagen-coated Bioflux microfluidic channels at a shear rate of 1000 or 1900  $\text{seconds}^{-1}$  for 4 minutes. Channels were washed with HEPEs-Tyrode buffer for 4 minutes at the same shear rate, and images were acquired by differential interface contrast (DIC) and fluorescence microscopy at  $\times 10$  on a Leica DMIRE2 deconvolution microscope. The width of the channel indicated by the dashed arrows is 350  $\mu\text{m}$ . Images are representative of 3 to 5 independent experiments. **B**, Platelet adhesion at shear rates of 1000  $\text{seconds}^{-1}$  was quantified with Bioflux 200 analysis software. **C**, Platelet adhesion at shear rates of 1900  $\text{seconds}^{-1}$  was quantified as in **B**. Data are expressed as mean  $\pm$  SEM from 3 to 5 independent experiments. \* $P < 0.05$ ; \*\* $P < 0.01$ .

activated Rac1 5-fold and Cdc42 4-fold (Rac1: fibrinogen,  $0.85 \pm 0.25$  arbitrary units [AU] versus basal,  $0.18 \pm 0.04$  AU,  $P < 0.05$ ; Cdc42: fibrinogen,  $1.46 \pm 0.35$  AU versus basal,  $0.37 \pm 0.08$  AU,  $P < 0.05$ ; Figure 4A and 4B). Slit2 did not affect basal levels of activated Rac1 and Cdc42 (Rac1: control,  $0.18 \pm 0.05$  AU versus Slit2,  $0.20 \pm 0.04$  AU; Cdc42: control,  $0.37 \pm 0.08$  AU versus Slit2,  $0.56 \pm 0.08$  AU; Figure 4A and 4B). Slit2 did not prevent activation of Rac1 or Cdc42 during fibrinogen-induced platelet spreading (Rac1: control,  $0.85 \pm 0.25$  AU versus Slit2,  $0.72 \pm 0.14$  AU; Cdc42: control,  $1.46 \pm 0.35$  AU versus Slit2,  $1.10 \pm 0.20$  AU; Figure 4A and 4B). These data suggest that Slit2 does not inhibit platelet spreading by preventing activation of Rac1 or Cdc42, nor did it prevent activation of these Rho-family GTPases during platelet spreading

### Slit2 Suppresses Activation of Akt, But Not Extracellular Signal-Regulated Kinase or p38 Mitogen-Activated Protein Kinase, During Platelet Spreading

Adhesion of platelets also involves activation of several major kinase pathways, namely p38 mitogen-activated protein kinase (MAPK), extracellular signal-regulated kinase (ERK), and Akt.<sup>21–25</sup> As expected, platelet spreading on fibrinogen resulted in a significant increase in phosphorylation of p38 MAPK, ERK, and Akt (p38 MAPK: fibrinogen,  $1.68 \pm 0.39$  AU versus basal,  $0.52 \pm 0.12$  AU,  $P < 0.05$ ; ERK: fibrinogen,  $0.76 \pm 0.16$  AU versus basal,  $0.18 \pm 0.02$  AU,  $P < 0.01$ ; Akt: fibrinogen,  $1.06 \pm 0.32$  AU versus basal,  $0.13 \pm 0.03$  AU,  $P < 0.01$ ; Figure 4C and 4E). Slit2 treatment had no effect on the basal level of kinase activation (p38 MAPK: control,  $0.52 \pm 0.12$  AU versus Slit2,  $0.48 \pm 0.12$  AU; ERK: control,  $0.18 \pm 0.02$  AU versus Slit2,  $0.29 \pm 0.11$  AU; Akt: control,  $0.13 \pm 0.03$  AU versus Slit2,  $0.14 \pm 0.04$  AU; Figure 4C and 4E). Slit2 had no effect on phosphorylation of p38 MAPK or ERK (p38 MAPK: control,  $1.68 \pm 0.39$  AU versus Slit2,  $1.25 \pm 0.34$  AU; ERK:

control,  $0.76 \pm 0.16$  AU versus, Slit2  $0.56 \pm 0.12$  AU; Figure 4C and 4D). In contrast, Slit2 significantly inhibited activation of Akt (control,  $1.06 \pm 0.32$  AU versus Slit2,  $0.34 \pm 0.07$  AU;  $P < 0.05$ ; Figure 4E).

Because activation of Akt is a key event in platelet secretion of  $\alpha$ -granules, we next tested the effects of Slit2 on this process.<sup>21,25,26</sup> We found that during platelet activation with ADP, Slit2 inhibited translocation of CD62P to the platelet surface ( $P < 0.05$ ; Figure IV in the online-only Data Supplement). Collectively, these data suggest that Slit2 inhibits platelet spreading by suppressing activation of Akt and furthermore that Slit2 prevents platelet activation and release of  $\alpha$ -granule contents.

### Slit2 Prolongs Bleeding Time In Vivo

We have observed that Slit2 inhibits platelet adhesion, spreading, and activation in vitro. To determine the possible effects of Slit2 on platelet function in vivo, we used the well-described murine tail bleeding model. After intravenous administration of vehicle to CD1 mice, bleeding time was  $24.3 \pm 2.7$  seconds (Figure 5A). After administration of Slit2 at doses of 1 and 1.8  $\mu\text{g}$  per mouse, the bleeding time was significantly prolonged to  $61.5 \pm 9.5$  and  $69.8 \pm 8.9$  seconds, respectively (1  $\mu\text{g}$  Slit2,  $P < 0.05$  versus vehicle; 1.8  $\mu\text{g}$  Slit2,  $P < 0.01$  versus vehicle). To verify these observations, the hemoglobin content of the saline into which the amputated tails were immersed was quantified by measuring absorbance at 575 nm. After administration of vehicle, the absorbance was  $0.12 \pm 0.01$  (Figure 5B) and rose to  $0.20 \pm 0.01$  ( $P < 0.01$  versus vehicle; Figure 5B) for 1.0  $\mu\text{g}$  Slit2 and to  $0.22 \pm 0.02$  ( $P < 0.01$  versus vehicle; Figure 5B) for 1.8  $\mu\text{g}$  Slit2. Administration of Slit2-N prolonged bleeding time in a dose-dependent manner, with bleeding time prolonged by 10-fold at the highest dose of Slit2-N administered (vehicle,  $27.6 \pm 6.5$  seconds versus Slit2, 1.8  $\mu\text{g}$   $274.5 \pm 76.9$  seconds;  $P < 0.01$ ; Figure 5C). When administered to mice of a different strain, namely C57BL/6, Slit2-N also prolonged

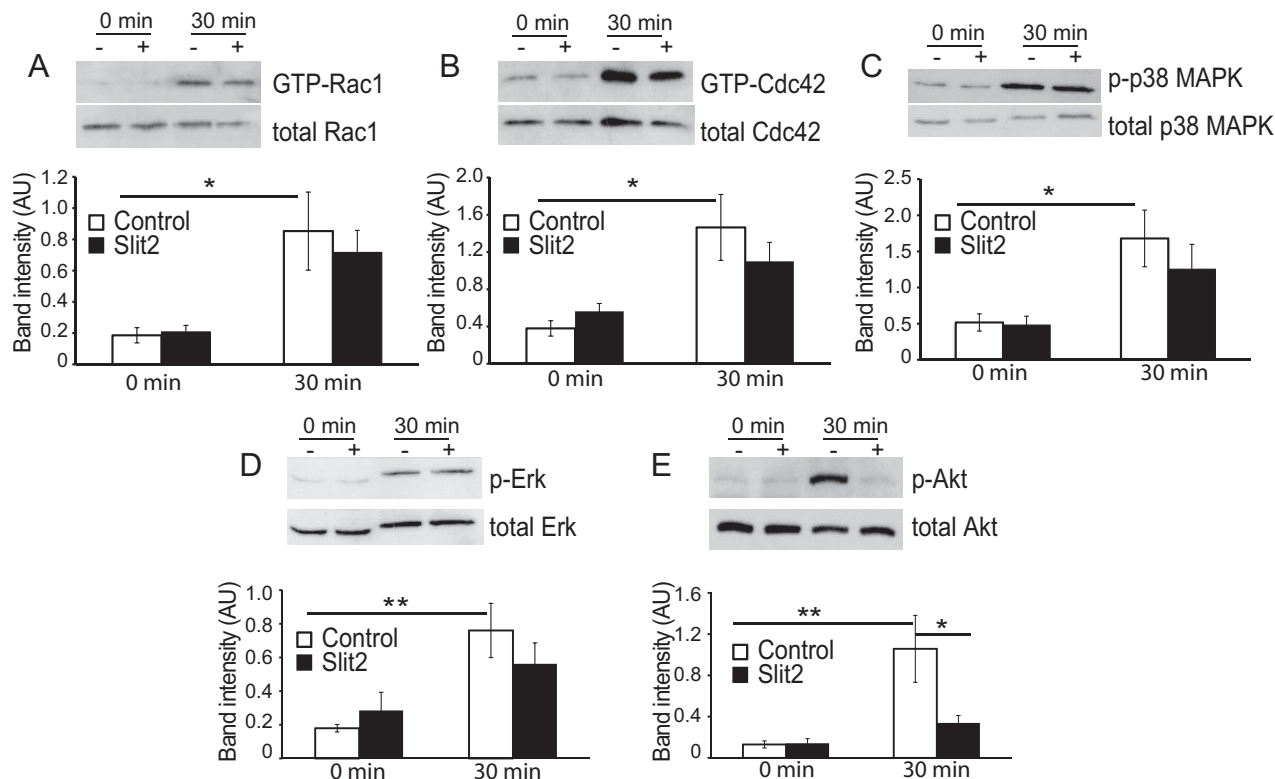


**Figure 4.** Slit2 inhibits activation of Akt but not Rac1, Cdc42, extracellular signal-regulated kinase (ERK), or p38 mitogen-activated protein kinase (MAPK). **A** through **E**, Washed human platelets were preincubated with Slit2 (4.5  $\mu\text{g}/\text{mL}$ ) or an equal volume of PBS (control) for 10 minutes at 37°C and allowed to spread on fibrinogen-coated wells for 30 minutes. Wells were washed with PBS to remove nonadherent platelets, and cell lysates were harvested from adherent platelets. **A**, Cell lysates were incubated with glutathione-S-transferase-p21-binding domain (GST-PBD) glutathione beads to immunoprecipitate activated Rac1, and immunoblotting was performed with anti-Rac1 antibody. Bottom, Band intensities of GTP-Rac1 normalized to total Rac1 expressed as mean  $\pm$  SEM from 5 independent experiments. **B**, Cell lysates were incubated with GST-PBD glutathione beads to immunoprecipitate activated Cdc42, and immunoblotting was performed with anti-Cdc42 antibody. Bottom, Band intensities of GTP-Cdc42 normalized to total Cdc42 expressed as mean  $\pm$  SEM from 6 independent experiments. **C**, Immunoblotting was performed with anti-phospho (p)-p38 MAPK antibody. Blots were stripped and reprobed with antibody detecting total p38 MAPK. Bottom, Band intensities of p-p38 MAPK normalized to total p38 MAPK expressed as mean  $\pm$  SEM from 7 independent experiments. **D**, Experiments were performed as in **C** with anti-p-ERK and anti-total ERK antibodies. Mean  $\pm$  SEM from 8 independent experiments. **E**, Experiments were performed as in **C** with anti-p-Akt and anti-total Akt antibodies. Mean  $\pm$  SEM from 4 independent experiments. \* $P < 0.05$ ; \*\* $P < 0.01$ .

bleeding times (vehicle,  $24.0 \pm 4.5$  seconds versus Slit2-N,  $51.1 \pm 6.3$  seconds;  $P < 0.05$ ; Figure VA in the online-only Data Supplement) and increased hemoglobin loss (vehicle,  $0.07 \pm 0.01$  versus Slit2-N,  $0.17 \pm 0.03$ ;  $P < 0.05$ ; Figure VB in the online-only Data Supplement). The specificity of Slit2-induced responses was verified by administering either Slit2-N together with a specific antagonist, RoboN, or Slit $\Delta$ D2, which lacks the Robo-1-binding domain. The observed bleeding time in mice given Slit2-N together with RoboN or Slit $\Delta$ D2 did not differ from that of vehicle-treated mice (vehicle,  $24 \pm 4.5$  seconds; Slit2-N+RoboN,  $24.9 \pm 5.4$  seconds; Slit $\Delta$ D2,  $18.7 \pm 2.7$  seconds; Figure VA in the online-only Data Supplement). In contrast, administration of either Slit2-N with RoboN or Slit $\Delta$ D2 resulted in a significantly shorter bleeding time than after administration of Slit2-N alone ( $P < 0.05$ ; Figure VA in the online-only Data Supplement). The corresponding hemoglobin loss was significantly greater in mice treated with Slit2-N compared with mice treated with Slit2-N and RoboN or with Slit $\Delta$ D2 (Slit2-N,  $0.17 \pm 0.03$ ; Slit2-N+RoboN,  $0.10 \pm 0.03$ ; Slit $\Delta$ D2,  $0.08 \pm 0.01$ ;  $P < 0.05$  versus Slit2-N; Figure VB in the online-only Data

Supplement). Together, these results indicate that Slit2 potently and specifically inhibits platelet-mediated hemostasis in vivo.

### Slit2 Inhibits In Vivo Formation of Stable, Occlusive Thrombi After Vascular Injury

To test the effects of Slit2 in a more clinically relevant context, namely in acute thrombosis, we used well-established murine models of mesenteric arteriole thrombosis and carotid artery thrombosis.<sup>27,28</sup>

After administration of vehicle, we performed intravital microscopy of mesenteric arterioles in mice and saw that single platelets deposited on the injured site of the vessel wall, forming multiple visible platelet aggregates and visible thrombi after several minutes of injury (Figure 6A). In Slit2-N-treated mice, a trend toward prolongation of vessel occlusion time was observed compared with vehicle-treated mice (vehicle,  $19.5 \pm 1.5$  minutes versus Slit2,  $28.1 \pm 3.6$  minutes;  $P = 0.051$ ; Figure 6A and 6B). In all vehicle-treated mice, the thrombi initially formed grew continuously to completely occlude the injured vessel (Figure 6A and 6B and Video V in the online-only Data Supplement). No significant thrombus dissociation, resulting in release of platelet emboli,

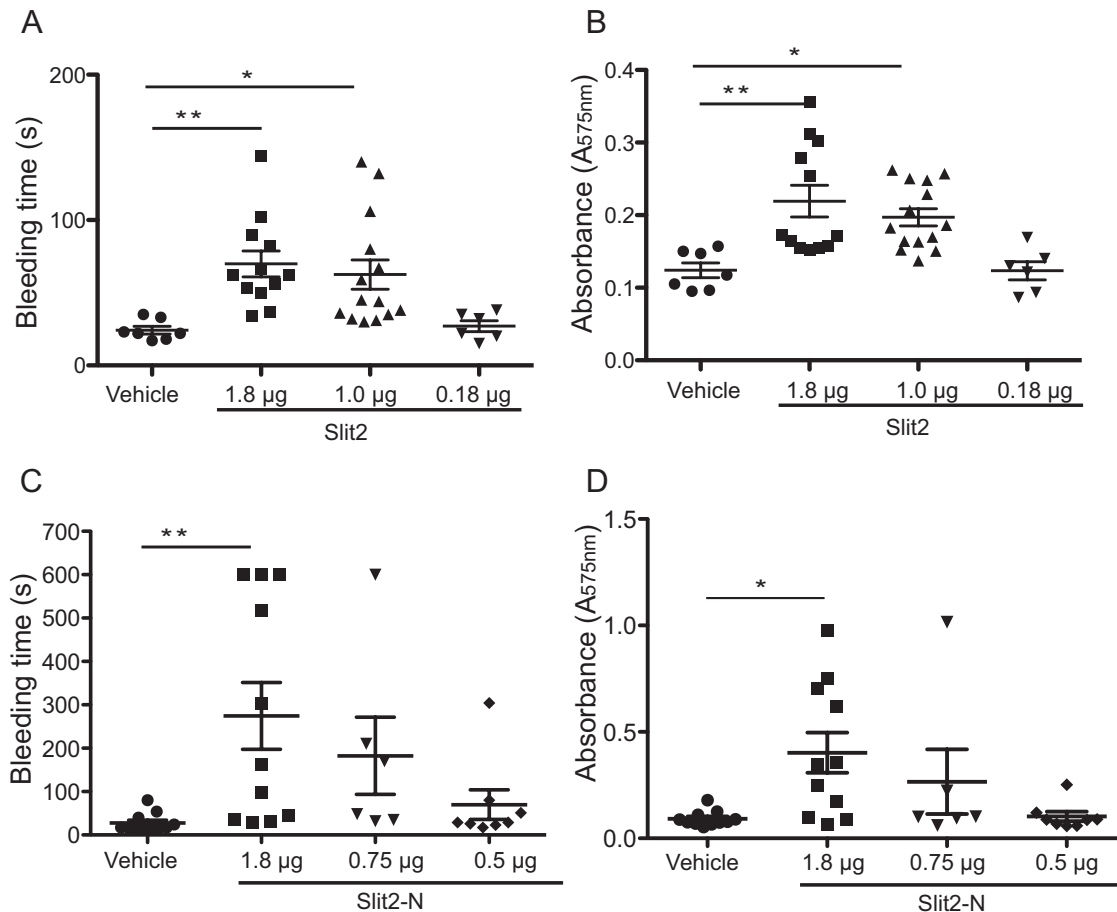


**Figure 5.** Slit2 increases bleeding time in vivo. CD1 mice were injected intravenously with the indicated dose of Slit2 or vehicle (0.9% NaCl). Two hours later, 5 mm of the distal tail was transected and immediately immersed in prewarmed saline. **A**, Bleeding times for mice from vehicle control and Slit2 treatment groups. Data are expressed as mean  $\pm$  SEM for 6 to 15 mice from each group. **B**, Blood loss from each mouse was quantified by measuring the hemoglobin content of the saline in which the tails were immersed. Hemoglobin content was determined by measuring absorbance at 575 nm. Data are expressed as mean  $\pm$  SEM. **C**, Experiments were conducted as in **A** using recombinant mouse truncated N-terminal Slit2 (Slit2-N) administered at the indicated doses. Data are expressed as mean  $\pm$  SEM for 6 to 12 mice from each group. **D**, Experiments were conducted as in **B** after administration of Slit2-N at the indicated doses. Data are expressed as mean  $\pm$  SEM for 6 to 12 mice from each group. \* $P$  < 0.05; \*\* $P$  < 0.01.

was observed during growth of the thrombi (Figure 6C). In contrast, after administration of Slit2-N, 5 of 7 mice formed thrombi that occluded the vessel and quickly dissociated, resulting in release of downstream emboli (vehicle,  $5 \pm 1$  versus Slit2,  $26 \pm 5$ ;  $P$  < 0.005; Figure 6C and Video V in the online-only Data Supplement) and partial reopening of occluded arterioles (Figure 6A and 6D and Video V in the online-only Data Supplement). In the remaining 2 Slit2-N-treated mice, thrombus formation was observed but complete vessel occlusion never occurred. At the end of the observation period (40 minutes), vessels remained partially open in none of the vehicle-treated mice but in all of the Slit2-N-treated mice ( $P$  < 0.05; Figure 6D).

We next tested the effects of Slit2 in a model that more closely mimics acute stroke in humans, namely carotid artery thrombosis. Once again, Slit2-treated mice exhibited a significant delay in vessel occlusion times compared with the group treated with Slit $\Delta$ D2 (Slit2-N,  $14.0 \pm 1.3$  minutes versus Slit $\Delta$ D2,  $10.6 \pm 0.6$  minutes;  $P$  < 0.05; Figure 6E). Collectively, these data demonstrate that Slit2 specifically prevents the formation of stable, occlusive arteriolar thrombi.

## Discussion

The soluble protein Slit2, interacting with its transmembrane receptor Robo-1, was first described in *Drosophila* as a neuronal and axonal repellent during development of the central nervous system.<sup>7-9</sup> Since then, Slit2 has been shown to inhibit chemotaxis of leukocytes and VSMCs toward a number of attractant cues associated with critical events in the progression of vascular lesions.<sup>10,12-15</sup> However, the effect of Slit2 on platelet functions has previously been unexplored. In this study, we demonstrate the unexpected ability of Slit2/Robo-1 interactions to inhibit several aspects of platelet adhesion, activation, and thrombus formation in vitro and in vivo. The antithrombotic properties of Slit2 point to its use as a potent agent capable of simultaneously preventing the vascular inflammation, neointimal proliferation, and thrombus formation that collectively result in occlusion of diseased vessels.

Although neuronal guidance cues belonging to the semaphorin and ephrin families have been implicated in leukocyte migration and platelet function, their precise role is unclear. Indeed, ephrins and semaphorins have been reported to both

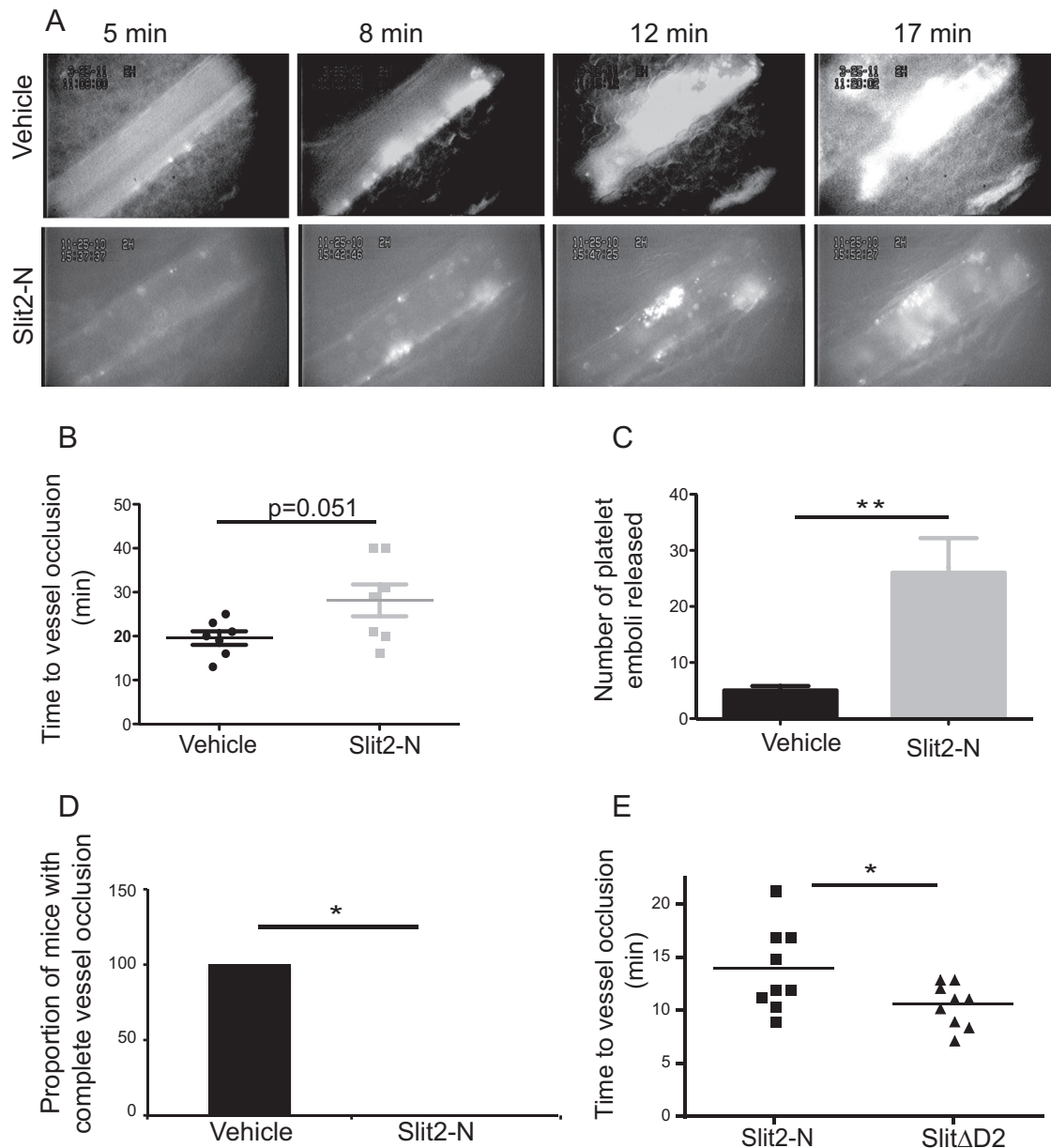


**Figure 6.** Slit2 inhibits in vivo formation of stable, occlusive thrombi after vascular injury. **A** through **D**, N-terminal Slit2 (Slit2-N; 1.8  $\mu$ g), Slit $\Delta$ D2, or vehicle was administered by tail-vein injection to C57BL/6 mice. Two hours later, mice were intravenously injected with donor-matched calcein-labeled platelets. The mesenteric vascular bed was exteriorized, and a section of arteriole was injured by superfusion with FeCl<sub>3</sub> (250 mmol/L). **A**, Thrombus formation was videorecorded and images were acquired at the indicated time points. **B**, Time to occlusion of the mesenteric arteriole was recorded. **C**, The number of emboli (>20  $\mu$ m) released during the 40-minute observation period after FeCl<sub>3</sub> vessel injury. **D**, Proportion of mice with complete arteriolar occlusion 40 minutes after FeCl<sub>3</sub> superfusion. **E**, After administration of Slit2-N or Slit $\Delta$ D2, the carotid artery was injured with 10% FeCl<sub>3</sub>, and the time to vessel occlusion was recorded. \* $P$ <0.05; \*\* $P$ <0.005.

enhance and inhibit inflammation and platelet function.<sup>29–31</sup> Work from our group and others demonstrates that Slit2 inhibits inflammatory cell and VSMC recruitment both in vitro and in vivo.<sup>10,12–15</sup> Although Slit2 inhibits chemotactic migration of leukocytes and VSMCs, the underlying mechanisms are not well understood. We recently showed that Slit2 inhibits polarization of migrating cells by preventing activation-induced generation of actin filament free barbed ends, necessary for rapid actin polymerization at the leading edge of the cell.<sup>13,32</sup> These data are in keeping with observations from neuronal cells connecting Robo-1 to cytoskeletal

proteins, including Slit-Robo GTPase-activating protein-1 and Ena.<sup>33,34</sup>

Platelet adhesion and spreading also involve cytoskeletal stabilization and destabilization. Accordingly, we found that Slit2 inhibited platelet spreading on diverse substrates, including fibrinogen, fibronectin, and collagen. Because Slit2 is a large glycoprotein, we considered the possibility that it may directly bind to glycoprotein 1b $\alpha$ , the receptor for von Willebrand factor, on the surface of platelets, thereby blocking steric interactions between glycoprotein 1b $\alpha$  and von Willebrand factor.<sup>35</sup> To examine this possibility, we tested the effects of Slit2 on platelet

adhesion to von Willebrand factor. Slit2 did not inhibit platelet adhesion to von Willebrand factor, suggesting that the observed effects of Slit2 on platelet adhesion to collagen did not occur by direct binding of Slit2 to the glycoprotein 1b $\alpha$  receptor (Figure VI in the online-only Data Supplement).

Platelet adhesion and spreading depend on rapid phospholipid metabolism and activation of major kinase pathways, especially Akt, ERK, and p38 MAPK. We found that Slit2 did not inhibit activation of ERK or p38 MAPK during platelet spreading. Our results are supported by observations of human neutrophils, human granulocytic cells, and Jurkat T lymphocytes, in which Slit2 did not affect chemoattractant-induced activation of ERK or p38 MAPK.<sup>13,14</sup> In yet another study, Slit2 suppressed ERK activation in chemokine-stimulated breast cancer cells.<sup>11</sup>

Akt is a well-recognized downstream effector of phosphatidylinositol 3-kinase and has been shown to phosphorylate and activate glycoprotein IIb/IIIa, thereby regulating actin assembly and promoting platelet shape change and stable aggregation.<sup>21,25,26,36,37</sup> Accordingly, we found that Slit2 inhibited Akt activation during platelet adhesion and spreading. These results are in concordance with those of others, demonstrating that Slit2 suppresses activation of Akt in Jurkat T lymphocytes after chemokine stimulation.<sup>12</sup> Interestingly, Akt-deficient platelets have a defect in secretion that results in reduced fibrinogen binding and consequently impaired aggregation.<sup>25</sup> The differential effects of Slit2 on inducible kinase activity can be attributed to the different cell types used. Previous reports have involved stimulating cells with chemoattractants in solution, whereas our study focused on deciphering how Slit2 modulates signaling pathways during platelet adhesion and spreading on immobilized ligands. Our studies indicate that Slit2 may suppress platelet spreading in part by downregulating Akt activation by limiting integrin function.

Our studies further demonstrated that during platelet adhesion and spreading, activation of the small Rho-family GTPase, Cdc42, was not affected by Slit2. These data differ from studies in human neutrophils and brain tumor cells in which Slit2 inhibited cell migration by preventing activation of Cdc42.<sup>13,17,34,38</sup> In another report involving VSMCs, Slit2 inhibited cell chemotaxis but did not prevent Cdc42 activation.<sup>10,12</sup> We found that the formation of dynamic, motile platelet filopodia was unaffected by Slit2. These results are entirely in keeping with observations in platelets derived from Cdc42-deficient mice. In platelets lacking Cdc42, spreading on fibrinogen and filopodial formation are completely intact.<sup>39</sup>

Using time-lapse videomicroscopy, we observed that Slit2 inhibited formation of lamellipodia during platelet adhesion and spreading. These effects are reminiscent of Rac1 deficiency. Indeed, platelets from Rac1-deficient mice display impaired lamellipodia formation and spreading on collagen but retain the ability to form filopodia.<sup>20</sup> Surprisingly, we did not find that Slit2 inhibited activation of Rac1 during platelet spreading. Emerging evidence points to Rac1 acting upstream of phosphatidylinositol 3-kinase and hence Akt during platelet activation.<sup>40–42</sup> Thus, it is possible that Rac1 activation occurred acutely and transiently in early stages of platelet

adhesion and spreading. Additionally, secondary platelet agonist receptors such as those of P2Y<sub>12</sub> and thromboxane A<sub>2</sub> are known to activate phospholipase C and downstream signaling pathways that activate Rac1.<sup>43</sup> Thus, the positive feedback loop and ambiguity in multiple signaling pathways generated by secondary platelet mediators may have masked the effects of Slit2 (Figure VII in the online-only Data Supplement).

We found that during ADP-mediated activation, Slit2 inhibited CD62P translocation to the surface of human platelets. These results are in keeping with work from other groups identifying a central role for Akt in platelet granular secretion.<sup>21,25,26</sup> Our findings are also in agreement with a recent study showing that Cdc42 is not required for  $\alpha$ -granule secretion.<sup>39</sup>

An intriguing question is how soluble levels of Slit2 vary in health and disease, particularly in the setting of cardiovascular disease. At a whole-organ level, Slit2 production has been demonstrated in brain, kidney, lung, and heart.<sup>14</sup> Cell types that have been shown to produce Slit2 include arterial endothelial cells, VSMCs, and fibroblasts.<sup>10,14</sup> Perusal of the Plasma Proteome Database (<http://www.plasmaproteomedata.org/index.html>) indicates that both Slit2 and Robo-1 have been detected in human plasma. However, the regulation of the physiological secretion of Slit2 has yet to be explored. Future studies examining the levels of Slit2 and Robo-1 in healthy subjects and in patients with cardiovascular disease will help to elucidate the mechanisms by which these proteins influence atherogenesis.

Of greatest significance, using well-established mouse models of tail bleeding, mesenteric arteriole thrombosis, and carotid artery thrombosis, we found that Slit2 impairs platelet function *in vivo*. Specifically, we found that administration of exogenous Slit2 impairs hemostasis and prevents formation of occlusive, stable thrombi in blood vessels subjected to acute injury. These findings point to the use of Slit2 as a potent new antiplatelet therapy to prevent the formation of thrombi that ultimately occlude vessels and cause myocardial or cerebral ischemia and infarction.<sup>1,2</sup> Our findings are even more compelling when one considers the distinct roles played by leukocytes, VSMCs, and platelets in initiating and exacerbating vascular injury and atherosclerosis.<sup>1,2</sup> Given the variety of cells, responses, and molecular cues involved in acute vascular injury and atherothrombosis, it is unlikely that targeting a single pathological pathway such as leukocyte infiltration or platelet activation will provide comprehensive clinical benefit. Until now, a single therapy that simultaneously blocks the different pathological processes that cause vascular injury has proven elusive. We report here that Slit2 inhibits platelet adhesion, spreading, and activation, and previous reports have demonstrated that the same protein inhibits leukocyte recruitment and chemotactic VSMC migration.<sup>10,12–15</sup> These observations make Slit2 an exciting therapeutic candidate for the prevention and treatment of atherothrombosis and acute vascular injury.

### Acknowledgments

We thank Michael Woodside and Paul Paroutis for assistance with microscopy procedures. We are grateful to Annie Bang for assistance

with flow cytometry, Derek Stephens for assistance with statistical analyses, Dr Peter L. Gross and Ali Akram for their technical assistance with tail bleeding assays, and Sylvie Perret for providing reagents.

### Sources of Funding

This work was supported by the Canadian Institutes of Health Research (MOP-111083; Dr Robinson) and an Early Researcher Award from the Ministry of Research and Innovation, Government of Ontario (Dr Robinson). Dr Robinson holds a Canada Research Chair, Tier 2. Dr Kahr was supported by an operating grant from the Canadian Institutes of Health Research (MOP-81208). Dr Ni was supported by Heart and Stroke Foundation of Canada (grant T 6449).

### Disclosures

None.

### References

- Meadows TA, Bhatt DL. Clinical aspects of platelet inhibitors and thrombus formation. *Circ Res*. 2007;100:1261–1275.
- Libby P. Inflammation in atherosclerosis. *Nature*. 2002;420:868–874.
- Huo Y, Schober A, Forlow SB, Smith DF, Hyman MC, Jung S, Littman DR, Weber C, Ley K. Circulating activated platelets exacerbate atherosclerosis in mice deficient in apolipoprotein E. *Nat Med*. 2003;9:61–67.
- von Hundelshausen P, Weber C. Platelets as immune cells: bridging inflammation and cardiovascular disease. *Circ Res*. 2007;100:27–40.
- Gawaz M, Langer H, May AE. Platelets in inflammation and atherogenesis. *J Clin Invest*. 2005;115:3378–3384.
- Saederup N, Chan L, Lira SA, Charo IF. Fractalkine deficiency markedly reduces macrophage accumulation and atherosclerotic lesion formation in CCR2<sup>-/-</sup> mice: evidence for independent chemokine functions in atherogenesis. *Circulation*. 2008;117:1642–1648.
- Brose K, Bland KS, Wang KH, Arnott D, Henzel W, Goodman CS, Tessier-Lavigne M, Kidd T. Slit proteins bind Robo receptors and have an evolutionarily conserved role in repulsive axon guidance. *Cell*. 1999;96:795–806.
- Kidd T, Bland KS, Goodman CS. Slit is the midline repellent for the robo receptor in *Drosophila*. *Cell*. 1999;96:785–794.
- Kidd T, Brose K, Mitchell KJ, Fetter RD, Tessier-Lavigne M, Goodman CS, Tear G. Roundabout controls axon crossing of the CNS midline and defines a novel subfamily of evolutionarily conserved guidance receptors. *Cell*. 1998;92:205–215.
- Liu D, Hou J, Hu X, Wang X, Xiao Y, Mou Y, De Leon H. Neuronal chemorepellent Slit2 inhibits vascular smooth muscle cell migration by suppressing small GTPase Rac1 activation. *Circ Res*. 2006;98:480–489.
- Prasad A, Fernandis AZ, Rao Y, Ganju RK. Slit protein-mediated inhibition of CXCR4-induced chemotactic and chemoinvasive signaling pathways in breast cancer cells. *J Biol Chem*. 2004;279:9115–9124.
- Prasad A, Qamri Z, Wu J, Ganju RK. Slit-2/Robo-1 modulates the CXCL12/CXCR4-induced chemotaxis of T cells. *J Leukoc Biol*. 2007;82:465–476.
- Tole S, Mukovozov IM, Huang YW, Magalhaes MA, Yan M, Crow MR, Liu GY, Sun CX, Durocher Y, Glogauer M, Robinson LA. The axonal repellent, Slit2, inhibits directional migration of circulating neutrophils. *J Leukoc Biol*. 2009;86:1403–1415.
- Wu JY, Feng L, Park HT, Havlioglu N, Wen L, Tang H, Bacon KB, Jiang Z, Zhang X, Rao Y. The neuronal repellent Slit inhibits leukocyte chemotaxis induced by chemotactic factors. *Nature*. 2001;410:948–952.
- Kanellis J, Garcia GE, Li P, Parra G, Wilson CB, Rao Y, Han S, Smith CW, Johnson RJ, Wu JY, Feng L. Modulation of inflammation by slit protein in vivo in experimental crescentic glomerulonephritis. *Am J Pathol*. 2004;165:341–352.
- Howitt JA, Clout NJ, Hohenester E. Binding site for Robo receptors revealed by dissection of the leucine-rich repeat region of Slit. *EMBO J*. 2004;23:4406–4412.
- Werbowski-Ogilvie TE, Seyed Sadr M, Jabado N, Angers-Loustau A, Agar NY, Wu J, Bjerkvig R, Antel JP, Faury D, Rao Y, Del Maestro RF. Inhibition of medulloblastoma cell invasion by Slit. *Oncogene*. 2006;25:5103–5112.
- Morlot C, Thielens NM, Ravelli RB, Hemrika W, Romijn RA, Gros P, Cusack S, McCarthy AA. Structural insights into the Slit-Robo complex. *Proc Natl Acad Sci U S A*. 2007;104:14923–14928.
- Kroll M. Mechanisms of Coagulation. In: Kroll M, ed. *Manual of Coagulation Disorders*. Malden, MA: Wiley-Blackwell; 2001:1–8.
- McCarty OJ, Larson MK, Auger JM, Kalia N, Atkinson BT, Pearce AC, Ruf S, Henderson RB, Tybulewicz VL, Machesky LM, Watson SP. Rac1 is essential for platelet lamellipodia formation and aggregate stability under flow. *J Biol Chem*. 2005;280:39474–39484.
- Chen J, De S, Damron DS, Chen WS, Hay N, Byzova TV. Impaired platelet responses to thrombin and collagen in AKT-1-deficient mice. *Blood*. 2004;104:1703–1710.
- Lai CF, Chaudhary L, Fausto A, Halstead LR, Ory DS, Avioli LV, Cheng SL. Erk is essential for growth, differentiation, integrin expression, and cell function in human osteoblastic cells. *J Biol Chem*. 2001;276:14443–14450.
- Li Z, Zhang G, Feil R, Han J, Du X. Sequential activation of p38 and ERK pathways by cGMP-dependent protein kinase leading to activation of the platelet integrin alphaIIb beta3. *Blood*. 2006;107:965–972.
- Mazharian A, Roger S, Berrou E, Adam F, Kauskot A, Nurden P, Jandrot-Perrus M, Bryckaert M. Protease-activating receptor-4 induces full platelet spreading on a fibrinogen matrix: involvement of ERK2 and p38 and Ca<sup>2+</sup> mobilization. *J Biol Chem*. 2007;282:5478–5487.
- Woulfe D, Jiang H, Morgans A, Monks R, Birnbaum M, Brass LF. Defects in secretion, aggregation, and thrombus formation in platelets from mice lacking Akt2. *J Clin Invest*. 2004;113:441–450.
- Yin H, Stojanovic A, Hay N, Du X. The role of Akt in the signaling pathway of the glycoprotein Ib-IX induced platelet activation. *Blood*. 2008;111:658–665.
- Reheman A, Gross P, Yang H, Chen P, Allen D, Leytin V, Freedman J, Ni H. Vitronectin stabilizes thrombi and vessel occlusion but plays a dual role in platelet aggregation. *J Thromb Haemost*. 2005;3:875–883.
- Reheman A, Yang H, Zhu G, Jin W, He F, Spring CM, Bai X, Gross PL, Freedman J, Ni H. Plasma fibronectin depletion enhances platelet aggregation and thrombus formation in mice lacking fibrinogen and von Willebrand factor. *Blood*. 2009;113:1809–1817.
- Aasheim H-C, Delabie J, Finne EF. Ephrin-A1 binding to CD4<sup>+</sup> T lymphocytes stimulates migration and induces tyrosine phosphorylation of PYK2. *Blood*. 2005;105:2869–2876.
- Prevost N, Woulfe DS, Jiang H, Stalker TJ, Marchese P, Ruggeri ZM, Brass LF. Eph kinases and ephrins support thrombus growth and stability by regulating integrin outside-in signaling in platelets. *Proc Natl Acad Sci U S A*. 2005;102:9820–9825.
- Zhu L, Stalker TJ, Fong KP, Jiang H, Tran A, Crichton I, Lee EK, Neeves KB, Maloney SF, Kikutani H, Kumanogoh A, Pure E, Diamond SL, Brass LF. Disruption of SEMA4D ameliorates platelet hypersensitivity in dyslipidemia and confers protection against the development of atherosclerosis. *Arterioscler Thromb Vasc Biol*. 2009;29:1039–1045.
- Sun CX, Magalhaes MA, Glogauer M. Rac1 and Rac2 differentially regulate actin free barbed end formation downstream of the fMLP receptor. *J Cell Biol*. 2007;179:239–245.
- Bashaw GJ, Kidd T, Murray D, Pawson T, Goodman CS. Repulsive axon guidance: Abelson and Enabled play opposing roles downstream of the roundabout receptor. *Cell*. 2000;101:703–715.
- Wong K, Ren XR, Huang YZ, Xie Y, Liu G, Saito H, Tang H, Wen L, Brady-Kalnay SM, Mei L, Wu JY, Xiong WC, Rao Y. Signal transduction in neuronal migration: roles of GTPase activating proteins and the small GTPase Cdc42 in the Slit-Robo pathway. *Cell*. 2001;107:209–221.
- Wagner DD. Cell biology of von Willebrand factor. *Annu Rev Cell Biol*. 1990;6:217–246.
- Hartwig JH, Kung S, Kovacsics T, Janmey PA, Cantley LC, Stossel TP, Toker A. D3 phosphoinositides and outside-in integrin signaling by glycoprotein IIb-IIIa mediate platelet actin assembly and filopodial extension induced by phorbol 12-myristate 13-acetate. *J Biol Chem*. 1996;271:32986–32993.
- Kirk RI, Sanderson MR, Lerea KM. Threonine phosphorylation of the beta 3 integrin cytoplasmic tail, at a site recognized by PDK1 and Akt/PKB in vitro, regulates Shc binding. *J Biol Chem*. 2000;275:30901–30906.

38. Yiin JJ, Hu B, Jarzynka MJ, Feng H, Liu KW, Wu JY, Ma HI, Cheng SY. Slit2 inhibits glioma cell invasion in the brain by suppression of Cdc42 activity. *Neuro Oncol.* 2009;11:779–789.
39. Pleines I, Eckly A, Elvers M, Hagedorn I, Eliaoutou S, Bender M, Wu X, Lanza F, Gachet C, Brakebusch C, Nieswandt B. Multiple alterations of platelet functions dominated by increased secretion in mice lacking Cdc42 in platelets. *Blood.* 2010;115:3364–3373.
40. Pandey D, Goyal P, Dwivedi S, Siess W. Unraveling a novel Rac1-mediated signaling pathway that regulates cofilin dephosphorylation and secretion in thrombin-stimulated platelets. *Blood.* 2009;114:415–424.
41. Piechulek T, Rehlen T, Walliser C, Vatter P, Moepps B, Gierschik P. Isozyme-specific stimulation of phospholipase C-gamma2 by Rac GTPases. *J Biol Chem.* 2005;280:38923–38931.
42. Welch HCE, Coadwell WJ, Stephens LR, Hawkins PT. Phosphoinositide 3-kinase-dependent activation of Rac. *FEBS Lett.* 2003;546:93–97.
43. Barkalow KL, Falet H, Italiano JE Jr, van Vugt A, Carpenter CL, Schreiber AD, Hartwig JH. Role for phosphoinositide 3-kinase in Fc gamma RIIA-induced platelet shape change. *Am J Physiol Cell Physiol.* 2003;285:C797–C805.

### CLINICAL PERSPECTIVE

Complications of vascular injury and atherosclerosis are the leading cause of mortality and morbidity in the Western world. In atherosclerosis, infiltrating leukocytes and vascular smooth muscle cells cause progressive vascular narrowing. Platelet-mediated thrombosis ultimately causes complete vessel occlusion, resulting in heart attack or stroke. In animal models and human patients, individually blocking these events, eg, with antiplatelet therapy, is only partially effective. Another therapeutic strategy is to target these multiple cell types globally. Slit proteins act as developmental neuronal repellents, and Slit2, via an interaction with its receptor, Robo-1, impairs inflammatory recruitment of leukocytes and vascular smooth muscle cells. However, thus far, the role of Slit2 in modulating platelet functions has not been explored. We report here the novel finding that human and mouse platelets express Robo-1 on their surface, making platelets potentially Slit2-responsive cells. Using static and shear assays, we demonstrate that Slit2 impaired platelet adhesion and spreading on a variety of physiologically relevant extracellular matrix proteins. Mouse tail bleeding assays and intravital microscopy further demonstrated that Slit2 is a powerful negative regulator of platelet function *in vivo*, prolonging bleeding time and preventing thrombus formation in mice during arterial injury. Slit2 mediated these effects, in part, by suppressing activation of Akt but not Rac1, Cdc42, extracellular signal-regulated kinase, or p38 mitogen-activated protein kinase. These results, combined with the established ability of Slit2 to block chemotaxis of leukocytes and vascular smooth muscle cells, indicate that Slit2, a naturally occurring protein, has the potential to be broadly effective in preventing and treating atherothrombosis and vascular injury.

## **SUPPLEMENTAL MATERIAL**

### **SUPPLEMENTAL METHODS**

#### **Reagents and antibodies**

Horn collagen (Equine Type 1) was from Nycomed (Melville, NY), hirudin from Bayer Inc. (Toronto, ON), recombinant mouse truncated Slit2 (Slit2-N) from R&D Systems (Minneapolis, MN), recombinant human truncated Slit2 (Slit2-N) from PeproTech (Rocky Hill, NJ), human von Willebrand factor (VWF) from Haematologic Technologies Inc. (Vermont, USA), calcein acetoxymethyl ester from Molecular Probes (Burlington, Canada), and all other chemicals from Sigma-Aldrich (St.Louis, MO). The following antibodies were used: anti-Robo-1 (Abcam, Cambridge, MA and Rockland Immunochemicals, Inc, Gilbertsville, PA), AlexaFluor 647-conjugated anti-His6 (AbD Serotec, Raleigh, NC), PE-conjugated anti-CD62P (BD Biosciences, Mississauga, ON, Canada), FITC-conjugated anti-CD41 (BD BioSciences), and PE-conjugated anti-CD41 (BD BioSciences). Anti-Cdc42, anti-Rac1, anti-Erk, anti-phospho-Erk, anti-p38 MAPK, anti-phospho-p38 MAPK, anti-Akt, and anti-phospho-Akt antibodies were from Cell Signaling (Danvers, MA). AlexaFluor-conjugated antibodies were from Invitrogen (Burlington, Canada) and HRP-conjugated and DyLight-conjugated antibodies from Jackson ImmunoResearch Laboratories (Bar Harbor, ME). Large-scale expression and purification of full length human Slit2 was performed as described

1.

#### **Generation of Slit $\Delta$ D2 and RoboN expression plasmids**

Slit $\Delta$ D2 was cloned in pTT28 by deleting the second LRR domain of truncated Slit2 (Slit2-N) using restriction enzymes BsrGI and NheI. After deleting 210 amino acids (Q235-W444) of Slit2-N, a short synthesized linker corresponding to amino acids YTAGGSAGGSAGGSAGKL was inserted into BsrGI and NheI restriction sites.

RoboN, the soluble N-terminal region comprising of the first two immunoglobulin domains of Robo-1, was cloned in pTT28 using NheI and BamHI restriction sites <sup>2</sup>. Large-scale expression and purification of Slit2 $\Delta$ D2 and RoboN was performed as previously described for Slit2 <sup>1</sup>.

### **Isolation of human and murine platelets**

Whole blood (6 vol) was collected from healthy donors into acid citrate dextrose (ACD; 1 vol) and centrifuged at 160g for 10 min to obtain platelet-rich plasma (PRP). PRP was washed with PBS adjusted to pH 6.3 with ACD, and centrifuged at 800g for 10 min. Platelets were resuspended in HEPES (10 mM) modified Tyrode's buffer (136 mM NaCl, 2.7 mM KCl, 0.42 mM NaH<sub>2</sub>PO<sub>4</sub>, 19 mM NaHCO<sub>3</sub>, 0.35 Na<sub>2</sub>HPO<sub>4</sub>, 5.5 mM glucose, 1 mM CaCl<sub>2</sub>, 1 mM MgCl<sub>2</sub> pH 7.2). Human megakaryocytes were isolated as previously described <sup>3</sup>.

Murine blood collected by cardiac puncture in hirudin (20  $\mu$ g/ml) was centrifuged at 100g for 10 min. PRP was fixed using 4% paraformaldehyde, washed, and resuspended in HEPES-Tyrode's buffer.

### **Immunoblotting and immunofluorescence labeling**

Immunofluorescent labeling of washed platelets, and immunoblotting of cell lysates harvested from human megakaryocytes and mature platelets were performed using anti-Robo-1 antibody <sup>3,4</sup>.

In other experiments, platelets ( $2 \times 10^8$ /ml) were incubated with Slit2 for 10 min at 37°C, and dispensed onto fibrinogen-coated surfaces for 30 min. Lysates were harvested from adherent platelets using lysis buffer (50mM Tris pH7.5, 10% glycerol, 1% NP-40, 100mM NaCl, 5mM MgCl<sub>2</sub>, 1mM PMSF, 1x protease inhibitor cocktail, 0.2mM NaVO<sub>3</sub>, 1mM DTT). Proteins were separated by SDS-PAGE and immunoblotting performed using anti-phospho-Akt, phospho-Erk, or phospho-p38 MAPK antibodies.

### **Platelet adhesion and spreading assays**

Spreading assays were performed as previously described, with minor modifications <sup>5</sup>. Washed platelets ( $10^7$ /ml) were pre-incubated with Slit2, Slit $\Delta$ D2 or PBS for 10 min, and dispensed onto fibrinogen-, fibronectin, or collagen-coated glass coverslips <sup>1</sup>. In other conditions, equimolar concentrations of RoboN and Slit2 were pre-incubated for 30 min prior to incubation with platelets. Non-adherent cells were removed by washing. Adherent platelets were labeled with Alexa Fluor 488-conjugated phalloidin <sup>5</sup>. Cells were visualized using a spinning disc DMIRE2 confocal microscope (Leica Microsystems, Toronto, Canada). Fifteen images from random fields were acquired using a 63x or 100x objective lens (1.4 numerical aperture) equipped with a Hamamatsu back-thinned EM-CCD camera and a 1.5x magnification lens (Spectral Applied Research).

Platelet surface area was calculated using Volocity™ software.

To quantify the number of platelets adhering per unit surface area,  $5 \times 10^7$  platelets were labeled with calcein (1  $\mu$ M) and dispensed into fibronectin-coated wells of 96-well plates. Fluorescence of adherent platelets was read using a microplate reader, and the fluorescent reading per well was correlated to the platelet number using a standard curve.

### **Microfluidic adhesion assays**

Channels of the Bioflux microfluidic system (Fluxion Biosciences, CA) were coated with collagen or VWF (50  $\mu$ g/ml). Washed platelets ( $10^7$ /ml) were labeled with calcein-AM, pre-incubated with Slit2 or PBS, and flowed through the channels at constant shear rates of  $1000 \text{ s}^{-1}$  or  $1900 \text{ s}^{-1}$  for 4 min. Channels were washed at the same shear rates for 4 min, and images acquired on a Leica DMIRE2 deconvolution microscope (10x) or on a Nikon Eclipse Ti confocal microscope (15x). The surface area covered by adherent platelets was quantified using the Bioflux™ 200 software.

### **Rac1 and Cdc42 activation assays**

Following incubation with Slit2, washed platelets ( $1.2 \times 10^9$ /ml) were allowed to spread on fibrinogen-coated wells for 30 min. Activation of Rac1 and Cdc42 was tested using GST-PBD glutathione beads as previously described<sup>1</sup>. Briefly, the p21-binding domain (PBD; aa 67–150) of PAK1 was cloned into the pGEX-4T3 vector, and expressed as a GST fusion protein in BL21 (DE3)

*Escherichia coli* cells. The GST-PBD fusion protein was purified using glutathione sepharose 4B beads (GE Healthcare Bio-Sciences, Piscataway, NJ, USA). Protein-bound beads were aliquoted and stored at -80°C till use. Following incubation with Slit2 (4.5 µg/ml) or PBS, 0.5 ml washed platelets (8x10<sup>8</sup>/ml) were allowed to spread on fibrinogen-coated wells for 30 min. Non-adherent platelets were removed by washing twice with PBS and lysates obtained from adherent platelets using ice-cold lysis buffer (50mM Tris pH7.5, 10% glycerol, 1% NP-40, 100mM NaCl, 5mM MgCl<sub>2</sub>, 1mM PMSF, 1x protease inhibitor cocktail, 0.2mM NaVO<sub>3</sub>, 1mM DTT). Samples were centrifuged at 13000g for 5 minutes, and supernatants were added to GST-PBD glutathione beads (20 µg GST PBD/sample) for 1 h and washed three times with cold wash buffer (50 mM Tris, pH 7.5, 40 mM NaCl, 0.5% NP-40). Densitometry analysis was performed using ImageJ software.

### **Flow cytometry**

To assess cell surface CD62P mobilization, a marker of platelet activation, human platelet-rich plasma was pre-incubated with Slit2 (4.5 µg/ml) for 10 min, then with ADP (10 µM) for 1 min<sup>6</sup>. In some instances, platelets were incubated with Slit2 for 10 min prior to incubation with ADP. The samples were then fixed with equal volume of 1% paraformaldehyde for 30 min, washed once with FACS buffer (PBS with 0.3% BSA, 10 mM NaN<sub>3</sub>), and incubated with anti-CD62P-PE and anti-CD41-FITC antibody for 30 min. Flow cytometry was performed using a Becton-Dickinson LSR II flow cytometer (Becton-Dickinson) and BD FACSDiva

software. Subsequent analysis was performed using FlowJo software (Tree Star, Inc., Ashland, OR, USA).

To quantify the levels of Robo-1 present in human platelets,  $4 \times 10^6$  washed platelets were fixed in 1% paraformaldehyde, permeabilized with 0.05% Triton X-100 for 5 min and incubated with anti-human Robo-1 antibody for 45 min. Platelets were then incubated with DyLight 649-conjugated anti-rabbit IgG and PE-conjugated anti-CD41 antibody for 30 min. Analysis was performed using a Gallios flow cytometer (Beckman Coulter, Inc) with Kaluza™ software.

To directly detect Slit2 binding to Robo-1 receptors,  $10^7$  washed platelets were incubated with 6xHis tagged-Slit2-N (12  $\mu\text{g/ml}$ ) for 15 min. In other conditions, platelets were incubated with Slit2-N and RoboN at 1:1 or 1:2 molar ratios, with RoboN, or with Slit $\Delta$ D2 for 15 min. Samples were incubated with PE-conjugated anti-CD41 antibody and Alexa Fluor-647 conjugated anti-His6 antibody for 30 min and fixed in 1% paraformaldehyde. In some instances, platelets were activated with 10  $\mu\text{M}$  ADP in the presence or absence of Slit2-N for 10 min. Samples were incubated with PE-conjugated anti-CD62P antibody and Alexa Fluor 647-conjugated anti-His6 antibody for 30 min. Analysis was performed using a Gallios flow cytometer with Kaluza™ software.

### **Murine tail bleeding assays**

Animals were cared for in accordance with the Guide for the Humane Use and Care of Laboratory Animals. All protocols were approved by The Hospital for Sick Children Research Institute Animal Care Committee. Briefly, Slit2 (0-1.8

$\mu\text{g}/\text{mouse}$ ) was intravenously injected via tail vein in adult CD1 or C57BL/6 mice (Charles River Laboratories, Wilmington, MA). Two h later, mice were anesthetized using 2.5-5% isoflourane, and placed on a heating pad. Five mm of the distal tail was amputated, and the remaining tail immersed in pre-warmed 0.9% NaCl <sup>7</sup>. The time required for spontaneous bleeding to cease was recorded. The amount of bleeding was quantified by measuring the hemoglobin content in the pre-warmed saline <sup>7</sup>.

### ***In vivo* thrombosis experiments**

We used two models of vascular injury, namely ferric-chloride induced mesenteric arteriolar injury and ferric-chloride induced carotid artery injury as previously described <sup>8-10</sup>.

For intravital microscopy of mesenteric arterioles, three to four week old male C57BL/6 mice (The Jackson Laboratory, Bar Harbor, Maine) were used and all experimental procedures were conducted as approved by the Animal Care Committee of St. Michael's Hospital (Toronto, Canada). Briefly, mice were intravenously injected with truncated mouse Slit2 (Slit2-N; 1.8  $\mu\text{g}/\text{mouse}$ ) or vehicle (0.9% NaCl) 2 h prior to intravital microscopy. Mice were then intravenously injected with purified, donor-matched platelets labeled with calcein (1  $\mu\text{g}/\text{ml}$ ). Mice were kept anesthetized with 2.5% tribromoethanol (0.015 mL/g body weight), and the mesentery vascular bed was exteriorized. A single arteriole ( $\sim 100 \mu\text{m}$  diameter with a shear rate of  $\sim 1500\text{s}^{-1}$ ) was selected in each mouse. A section of arteriole of approximate diameter 2-5 mm was injured by

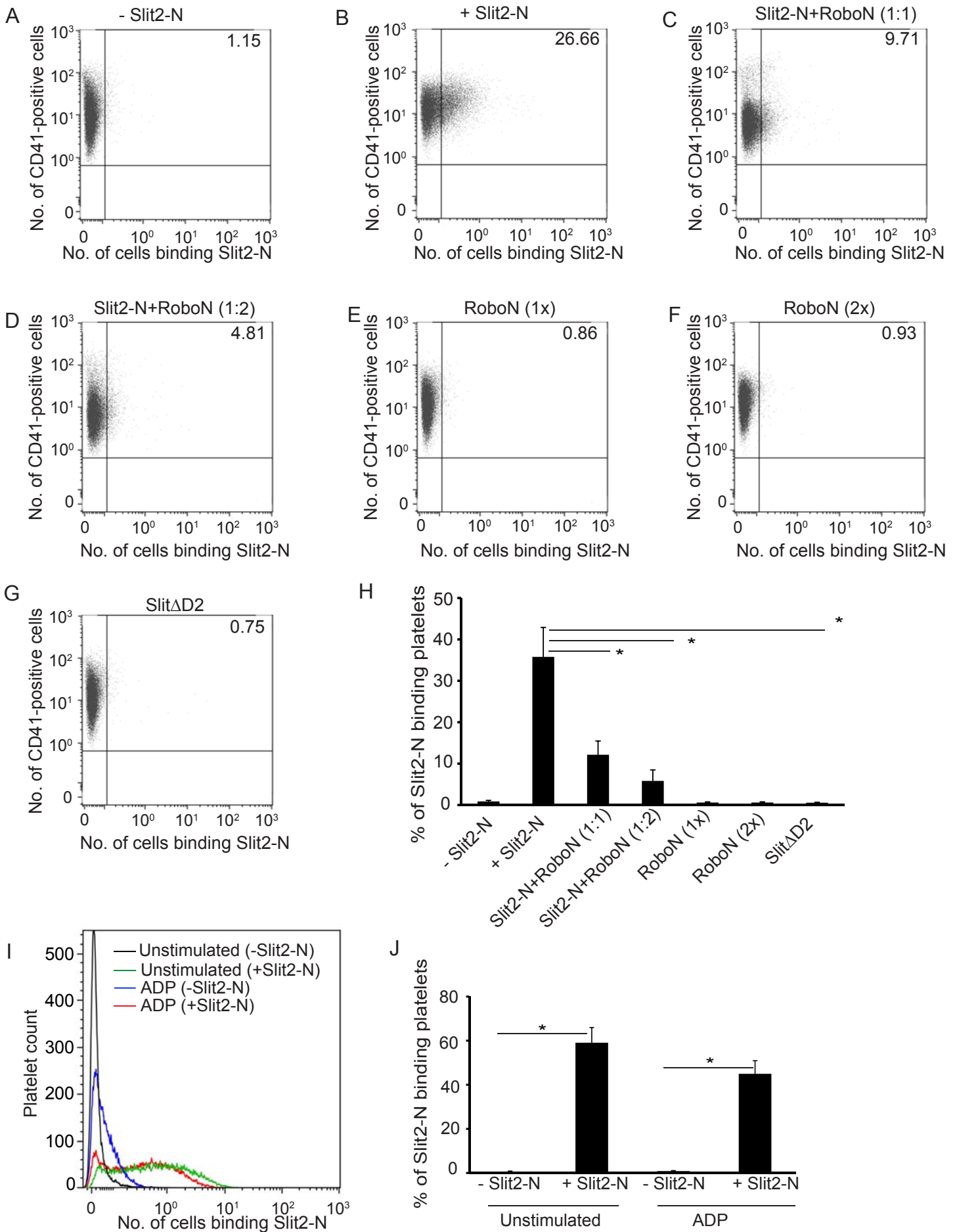
superfusion with 30  $\mu$ L of 250 mM FeCl<sub>3</sub> and thrombus formation was video-recorded using a Zeiss Axiovert 135-inverted fluorescent microscope (Zeiss Oberkochen, Germany). Thrombus formation and stability were assessed by measuring: (i) time to complete vessel occlusion (defined as the complete cessation of blood flow for >10 sec), (ii) the number of platelet emboli (>20  $\mu$ m) that disappeared from the viewing field, and (iii) the number of arterioles that re-opened after complete vessel occlusion.

For the carotid artery injury model, six week old-mice were anesthetized, the carotid artery was dissected and arterial injury was induced with a strip of Whatman filter paper saturated with 10% ferric chloride. The blood flow was monitored with a miniature Doppler flow probe (TS420 transit-time perivascular flowmeter, Transonic Systems Inc.) and time to vessel occlusion was measured (defined as cessation of blood flow for at least 3 min).

### **Statistical analysis**

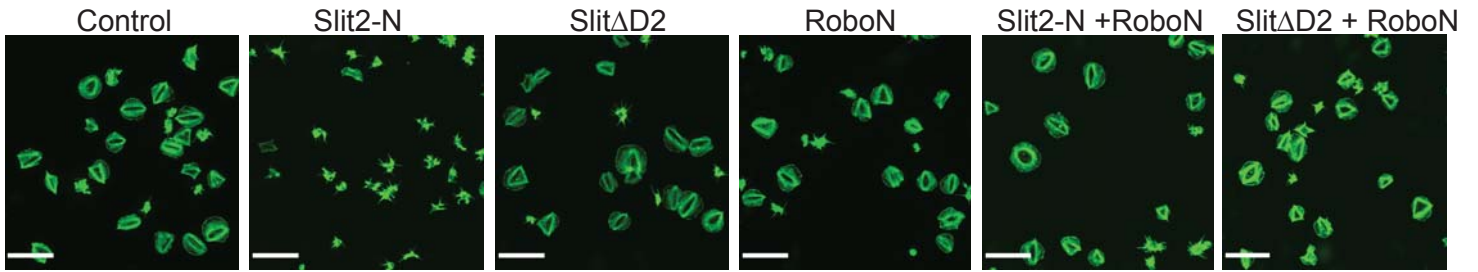
One-way or two-way analysis of variance followed by Bonferonni's (Figure 2, Figure 4, Figure S2, Figure S3) or, if comparisons were against a reference group, Dunnett's (Figure 5 and Figure S5) post-hoc testing was performed to compare group means in multiple comparisons.

Supplemental Figure 1. Slit2 binds to Robo-1 on the surface of platelets.

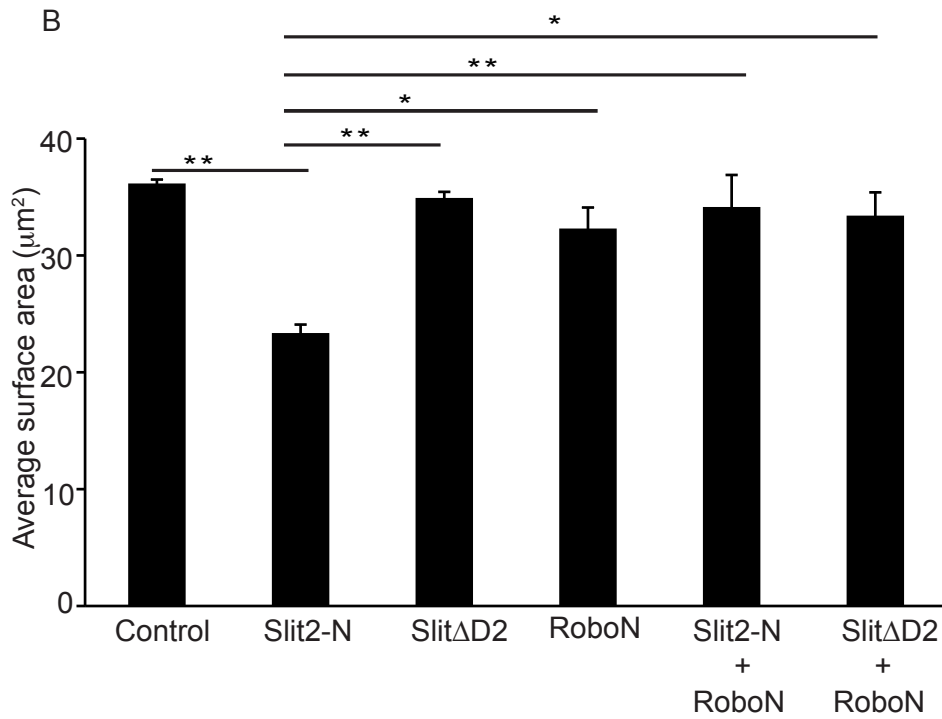


Supplemental Figure 2. Effects of Slit2-N, RoboN and SlitΔD2 on platelet spreading

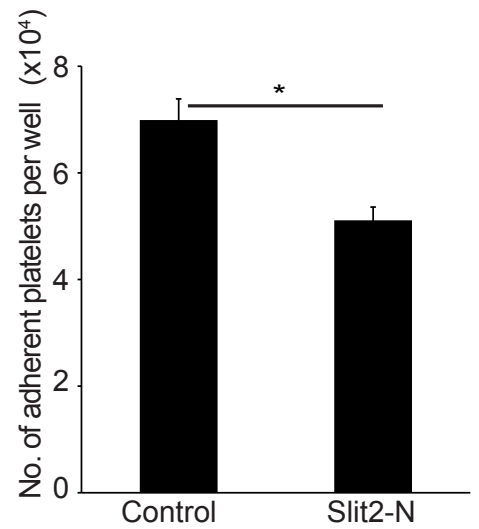
A



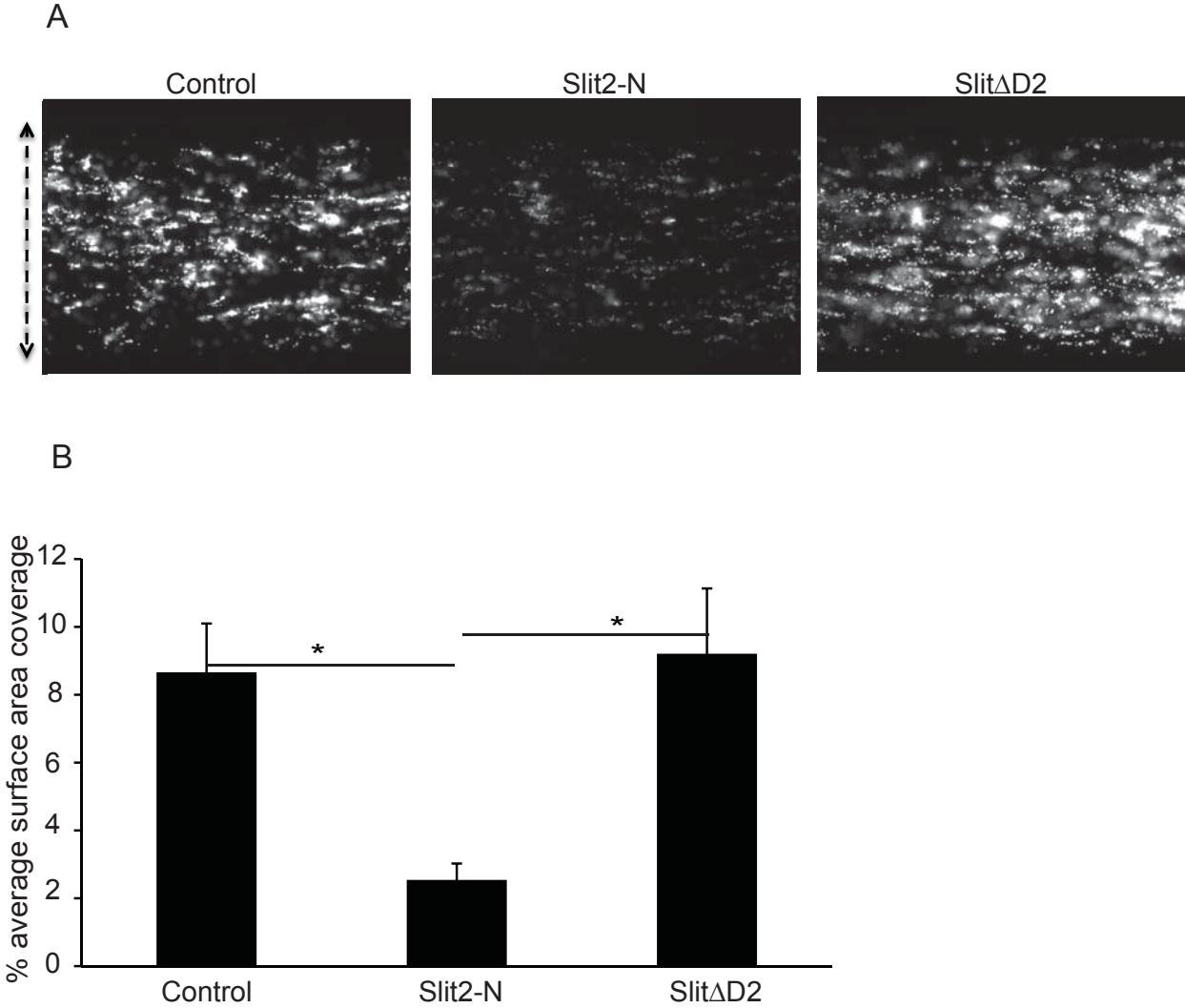
B



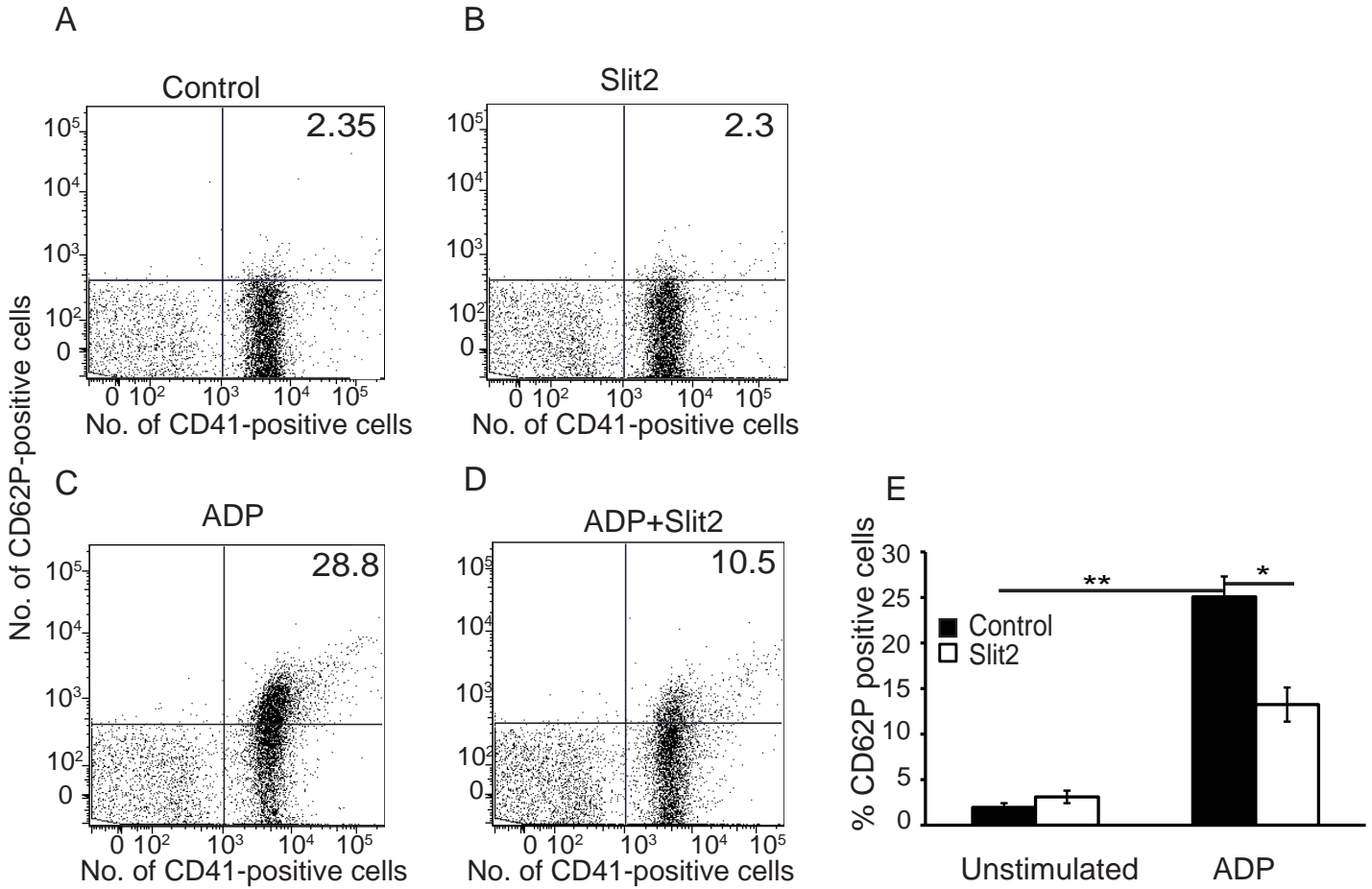
C



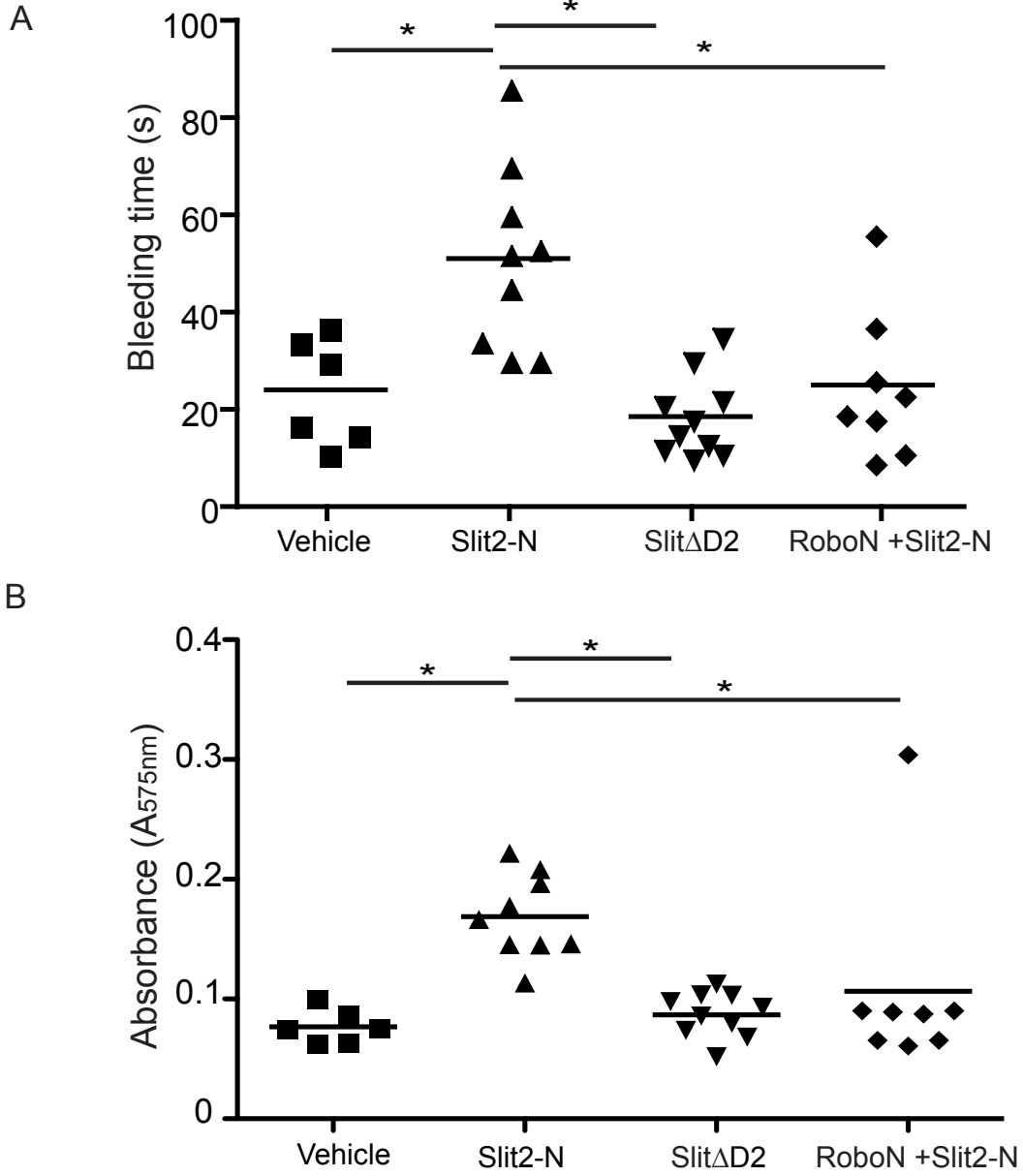
Supplemental Figure 3. Slit2 specifically inhibits platelet adhesion to collagen under shear flow conditions.



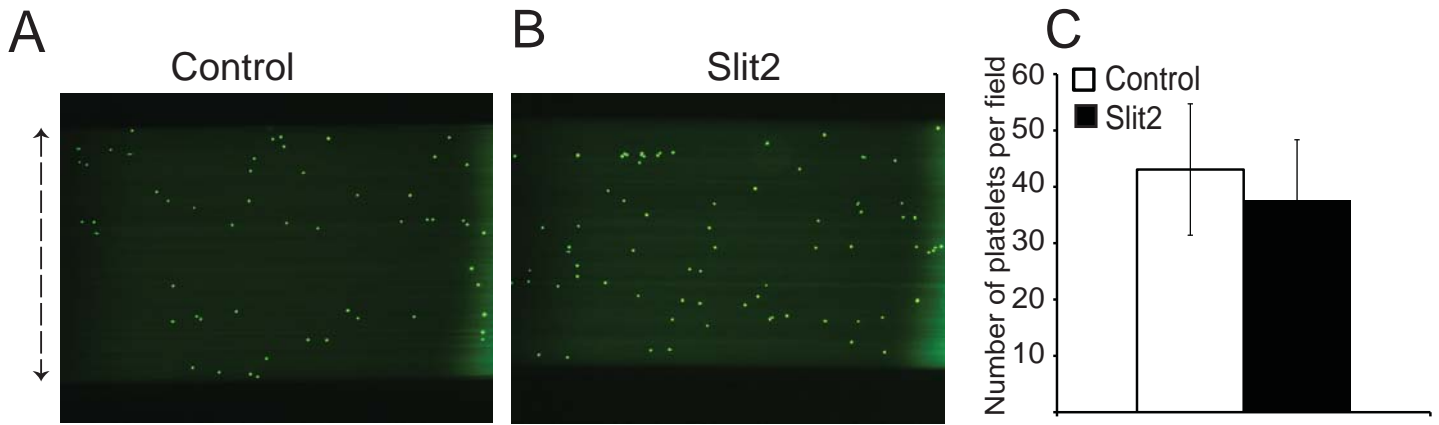
Supplemental Figure 4. Slit2 suppresses ADP-mediated platelet activation.



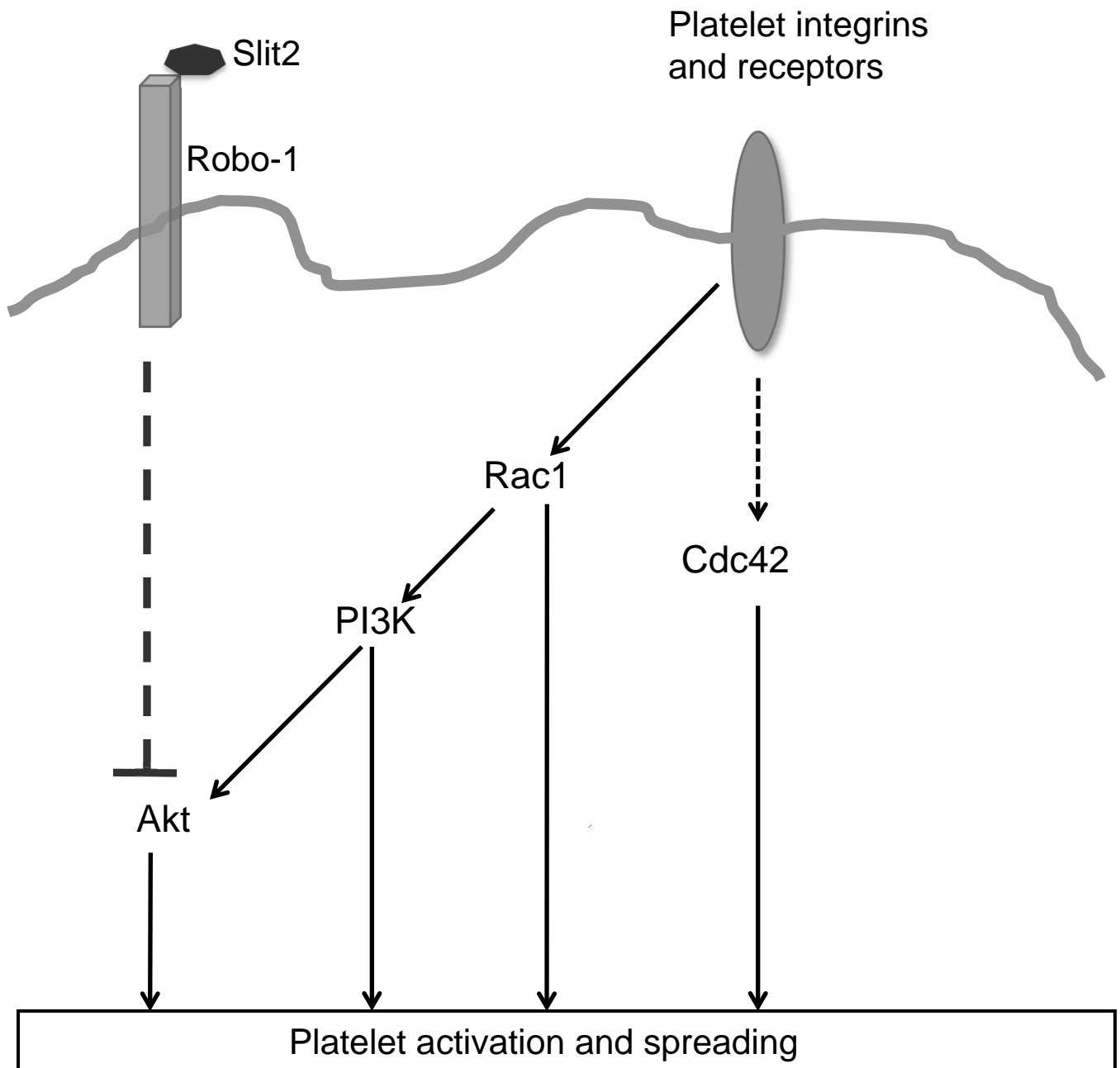
Supplemental Figure 5. Slit2 prolongs bleeding time *in vivo* in C57BL/6 mice



Supplemental Figure 6. Slit2 does not inhibit platelet adhesion to von Willebrand factor (VWF) under shear flow conditions



Supplemental Figure 7. Potential effects of Slit2/Robo-1 signaling on platelet activation



## SUPPLEMENTAL FIGURE LEGENDS

### Supplemental Figure 1. Slit2 binds to Robo-1 on the surface of platelets.

Washed platelets were incubated with His-tagged Slit2-N, RoboN, Slit $\Delta$ D2, or Slit2-N together with RoboN. Platelets were fixed and incubated with PE-conjugated anti-CD41 antibody and Alexa Fluor 647-conjugated anti-His6 antibody. **(A)** Surface labeling of platelets in the absence of Slit2-N. **(B)** Surface labeling of platelets after incubation with Slit2-N. **(C)** Surface labeling of platelets after incubation with Slit2-N and RoboN at equimolar ratio. **(D)** Surface labeling of platelets after incubation with Slit2-N and RoboN at 1:2 molar ratio. **(E)** Surface labeling of platelets after incubation with RoboN (1x molar ratio). **(F)** Surface labeling of platelets after incubation with RoboN (2x molar ratio). **(G)** Surface labeling of platelets after incubation with Slit $\Delta$ D2. Representative images of one from five similar independent experiments are shown. Numerical values indicate the percentage of cells with positive labeling. **(H)** Experiments were performed as in (A) to (G). Graph depicting the percentage of platelets demonstrating positive surface labeling, indicative of Slit2-N binding. Data are expressed as mean  $\pm$  SEM from 5 independent experiments. \*,  $p < 0.05$ . **(I)** Unstimulated or ADP-stimulated washed platelets were incubated with or without His-tagged Slit2-N. Platelets were fixed and incubated with PE-conjugated anti-CD62P antibody and Alexa Fluor 647-conjugated anti-His6 antibody. Histogram depicting the amount of Slit2-N binding. **(J)** Experiments were performed as in (I). Graph depicting the percentage of platelets demonstrating positive surface

labeling for Slit2-N. Data are expressed as mean  $\pm$  SEM from 3 independent experiments. \*,  $p < 0.05$

**Supplemental Figure 2. Effects of Slit2-N, RoboN, and Slit $\Delta$ D2 on platelet**

**spreading.** Washed human platelets ( $10^7$ /ml) were pre-incubated with Slit2-N (4.5  $\mu$ g/ml), Slit $\Delta$ D2 or an equal volume of PBS (control) for 10 min at 37°C.

Equimolar concentrations of Slit2-N and RoboN were pre-incubated together prior to addition to washed platelets. Cells were dispensed onto coverslips pre-coated with fibrinogen. **(A)** Following the indicated treatments, platelets adherent to fibrinogen were fixed, permeabilized, incubated with Alexa Fluor 488-conjugated phalloidin, and visualized using a Leica DMIRE2 spinning disc confocal microscope. Scale bars represents 16  $\mu$ m. **(B)** Experiments were performed as in (A). Images were acquired from 10 random fields and the surface area of platelets was quantified using Volocity<sup>TM</sup> software. Data are expressed as mean  $\pm$  SEM from 3 independent experiments. \*,  $p < 0.05$ ; \*\*,  $p < 0.01$ . **(C)** Calcein-labeled platelets ( $5 \times 10^7$ ) were allowed to adhere to fibronectin-coated wells of 96 well plates for 30 min. The fluorescence intensity of the adherent platelets was measured using a plate reader and the intensity correlated to the cell number using a standard curve. Data are expressed as mean  $\pm$  SEM from 4 independent experiments. \*,  $p < 0.01$ .

**Supplemental Figure 3. Slit2 specifically inhibits platelet adhesion to**

**collagen under shear flow conditions.** **(A)** Washed human platelets ( $10^7$ /ml)

were incubated with calcein-AM (4  $\mu$ M) for 20 min, washed, and incubated with Slit2-N, Slit $\Delta$ D2 or an equal volume of PBS (control) for 10 min at 37°C. Platelets were perfused over collagen-coated Bioflux™ micro-fluidic channels at constant shear rates of 1000 sec<sup>-1</sup> for 4 min. Channels were washed with HEPES-Tyrode's buffer for 4 min at the same shear rates and images acquired by fluorescence microscopy on a Nikon Eclipse Ti confocal microscope (15x). The width of the channel indicated by the dashed arrows is 350  $\mu$ m. Images are representative of 7-10 independent experiments. **(B)** Platelet adhesion to collagen-coated micro-fluidic channels was quantified using Bioflux™ 200 analytic software. Data are expressed as mean  $\pm$  SEM from 7-10 independent experiments. \*,  $p < 0.05$

**Supplemental Figure 4. Slit2 suppresses ADP-mediated platelet activation.**

Human platelet-rich plasma (PRP) was diluted with HEPES-Tyrode's buffer to a cell density of 10<sup>7</sup>/ml, and incubated with Slit2 (4.5  $\mu$ g/ml) or an equal volume of PBS (control) for 10 min at 37°C. Platelets were stimulated with ADP (10  $\mu$ M) for 1 min, fixed and incubated with PE-conjugated anti-CD62P antibody and FITC-conjugated anti-CD41 antibody. Flow cytometric analysis was performed using a Becton-Dickinson LSR II flow cytometer and FlowJo software. **(A)** Resting platelets (control). **(B)** Resting platelets incubated with Slit2. **(C)** Platelets stimulated with ADP. **(D)** Platelets pre-incubated with Slit2 prior to ADP stimulation. Representative images of one from three similar independent experiments are shown. Numerical values indicate percentage of platelets

positive for both surface CD62P and CD41. (E) Graph depicting the percentage of CD62P-positive resting platelets (control), resting platelets incubated with Slit2, platelets activated with ADP, and platelets pre-treated with Slit2 prior to activation with ADP. Data are expressed as mean  $\pm$  SEM from 3-5 independent experiments. \*,  $p < 0.01$ ; \*\*,  $p < 0.0001$ .

**Supplemental Figure 5. Slit2 prolongs bleeding time *in vivo* in C57BL/6**

**mice.** C57BL/6 mice were intravenously injected with Slit2-N (1.8  $\mu\text{g}/\text{mouse}$ ), Slit $\Delta$ D2, equimolar concentrations of Slit2-N and RoboN, or vehicle (0.9% NaCl). Two h later, 5 mm of the distal tail was transected and immediately immersed in pre-warmed saline. (A) Bleeding times for mice from the indicated experimental groups. (B) Hemoglobin content of the blood lost from each mouse as determined by measuring absorbance at 575 nm. Data are expressed as mean  $\pm$  SEM from 6-10 mice per treatment group. \*,  $p < 0.05$ .

**Supplemental Figure 6. Slit2 does not inhibit platelet adhesion to von**

**Willebrand factor (VWF) under shear flow conditions.** (A and B) Washed human platelets ( $3 \times 10^7/\text{ml}$ ) were incubated with calcein-AM (4  $\mu\text{M}$ ) for 20 min, washed, and incubated with Slit2 (B; 4.5  $\mu\text{g}/\text{ml}$ ) or an equal volume of PBS (A; control) for 10 min at 37 $^\circ$  C. Platelets were perfused over VWF-coated microfluidic channels (Bioflux<sup>TM</sup>) at constant shear rates of 1000  $\text{sec}^{-1}$  for 4 min. Images were acquired at 20x on a Nikon TE2000 inverted microscope. The width of the channel indicated by the dashed arrows is 350  $\mu\text{m}$ . Images are

representative of 3 independent experiments. (C) Mean number of platelets  $\pm$  SEM counted per 20x field from 3 independent experiments.

**Supplemental Figure 7. Potential effects of Slit2/Robo-1 signaling on platelet activation.** The signaling induced by Slit2 binding to Robo-1 on the platelet surface is presumed to inhibit Akt signaling, which may, in turn, inhibit platelet activation. Binding of ligands to platelet surface receptors activates Rac1, which, in turn, activates PI3K and Akt. In this way, Slit2 may prevent Akt-induced platelet adhesion and spreading without noticeable effects on Rac1 activation. PI3K, phosphatidylinositol 3-kinase

## SUPPLEMENTAL REFERENCES

1. Tole S, Mukovozov IM, Huang YW, Magalhaes MA, Yan M, Crow MR, Liu GY, Sun CX, Durocher Y, Glogauer M, Robinson LA. The axonal repellent, Slit2, inhibits directional migration of circulating neutrophils. *J Leukoc Biol.* 2009;86:1403-1415.
2. Morlot C, Thielens NM, Ravelli RB, Hemrika W, Romijn RA, Gros P, Cusack S, McCarthy AA. Structural insights into the Slit-Robo complex. *Proc Natl Acad Sci U S A.* 2007;104:14923-14928.
3. Lo B, Li L, Gissen P, Christensen H, McKiernan PJ, Ye C, Abdelhaleem M, Hayes JA, Williams MD, Chitayat D, Kahr WH. Requirement of VPS33B, a member of the Sec1/Munc18 protein family, in megakaryocyte and platelet alpha-granule biogenesis. *Blood.* 2005;106:4159-4166.
4. Licht C, Pluthero FG, Li L, Christensen H, Habbig S, Hoppe B, Geary DF, Zipfel PF, Kahr WH. Platelet-associated complement factor H in healthy persons and patients with atypical HUS. *Blood.* 2009;114:4538-4545.
5. Mazharian A, Roger S, Berrou E, Adam F, Kauskot A, Nurden P, Jandrot-Perrus M, Bryckaert M. Protease-activating receptor-4 induces full platelet spreading on a fibrinogen matrix: involvement of ERK2 and p38 and Ca<sup>2+</sup> mobilization. *J Biol Chem.* 2007;282:5478-5487.
6. Hagberg IA, Lyberg T. Blood platelet activation evaluated by flow cytometry: optimised methods for clinical studies. *Platelets.* 2000;11:137-150.

7. Cho J, Furie BC, Coughlin SR, Furie B. A critical role for extracellular protein disulfide isomerase during thrombus formation in mice. *J Clin Invest.* 2008;118:1123-1131.
8. Abou-Saleh H, Yacoub D, Theoret JF, Gillis MA, Neagoe PE, Labarthe B, Theroux P, Sirois MG, Tabrizian M, Thorin E, Merhi Y. Endothelial progenitor cells bind and inhibit platelet function and thrombus formation. *Circulation.* 2009;120:2230-2239.
9. Reheman A, Gross P, Yang H, Chen P, Allen D, Leytin V, Freedman J, Ni H. Vitronectin stabilizes thrombi and vessel occlusion but plays a dual role in platelet aggregation. *J Thromb Haemost.* 2005;3:875-883.
10. Reheman A, Yang H, Zhu G, Jin W, He F, Spring CM, Bai X, Gross PL, Freedman J, Ni H. Plasma fibronectin depletion enhances platelet aggregation and thrombus formation in mice lacking fibrinogen and von Willebrand factor. *Blood.* 2009;113:1809-1817.

## **SUPPLEMENTAL VIDEO LEGENDS**

### **Supplemental Video 1. Human platelets spread effectively on fibrinogen.**

Isolated human platelets ( $10^7$ /ml) were allowed to adhere to fibrinogen-coated glass coverslips in an Attafluor® cell chamber and placed on the heated stage of a Leica DMIRE2 deconvolution microscope at 100X magnification. Images were acquired every 10 s for up to 30 min using Volocity™ software interfaced with a Hamamatsu C4242-95-12ERG camera. Representative video from one of three separate experiments.

### **Supplemental Video 2. Slit2 inhibits spreading of human platelets on**

**fibrinogen.** Experiments were performed as described in ‘Supplemental Video 1’. Platelets were pre-incubated with Slit2 (4.5  $\mu$ g/ml) for 10 min, and cell spreading was monitored by time-lapse videomicroscopy. Representative video from one of three separate experiments.

### **Supplemental Video 3. Human platelets form aggregates on collagen-**

**coated surfaces under shear flow.** Calcein labeled (4 $\mu$ M) washed human platelets ( $10^7$ /ml) were perfused over collagen-coated micro-fluidic channels at constant shear rates of 1900  $\text{sec}^{-1}$  for 4 min. Image acquisition was performed using the Bioflux™ 200 software on a 10X objective (with 1.5X magnification lens) of a Nikon Eclipse Ti inverted confocal microscope. Images were acquired every 2 s for up to 4 min. Representative video from one of three separate experiments.

**Supplemental Video 4. Slit2 inhibits adhesion of human platelets to collagen-coated surfaces under shear flow.** Platelets were incubated with Slit2 (4.5  $\mu\text{g/ml}$ ) for 10 min and experiments performed as in 'Supplemental Video 3'. Representative video from one of three separate experiments.

**Supplemental Video 5. Slit2 impairs thrombus stability *in vivo*.**

C57BL/6 mice were intravenously injected with Slit2-N (1.8  $\mu\text{g/mouse}$ ) or vehicle (0.9% NaCl) 2 h prior to intravital microscopy. Donor-matched calcein-labeled platelets were then injected into the mice and anesthetized. The mesentery vascular bed was exteriorized and a section of the arteriole injured by  $\text{FeCl}_3$ . Thrombus formation was videorecorded using a Zeiss Axiovert fluorescent microscope. Representative video from one of seven separate experiments.

## The Cell Motility Modulator Slit2 Is a Potent Inhibitor of Platelet Function

Sajedabanu Patel, Yi-Wei Huang, Adili Rehemani, Fred G. Pluthero, Swasti Chaturvedi, Ilya M. Mukovozov, Soumitra Tole, Guang-Ying Liu, Ling Li, Yves Durocher, Heyu Ni, Walter H.A. Kahr and Lisa A. Robinson

*Circulation*. 2012;126:1385-1395; originally published online August 3, 2012;  
doi: 10.1161/CIRCULATIONAHA.112.105452

*Circulation* is published by the American Heart Association, 7272 Greenville Avenue, Dallas, TX 75231  
Copyright © 2012 American Heart Association, Inc. All rights reserved.  
Print ISSN: 0009-7322. Online ISSN: 1524-4539

The online version of this article, along with updated information and services, is located on the  
World Wide Web at:

<http://circ.ahajournals.org/content/126/11/1385>

Data Supplement (unedited) at:

<http://circ.ahajournals.org/content/suppl/2012/08/03/CIRCULATIONAHA.112.105452.DC1.html>

**Permissions:** Requests for permissions to reproduce figures, tables, or portions of articles originally published in *Circulation* can be obtained via RightsLink, a service of the Copyright Clearance Center, not the Editorial Office. Once the online version of the published article for which permission is being requested is located, click Request Permissions in the middle column of the Web page under Services. Further information about this process is available in the [Permissions and Rights Question and Answer](#) document.

**Reprints:** Information about reprints can be found online at:  
<http://www.lww.com/reprints>

**Subscriptions:** Information about subscribing to *Circulation* is online at:  
<http://circ.ahajournals.org/subscriptions/>